

p

RSRS

(NASA-CR-162967) AN ATLAS OF ALOUETTE 2  
IONOGRAMS RECORDED AT PORT STANLEY,  
SINGAPORE AND WINKFIELD DURING THE MONTH  
AFTER LAUNCH (Radio and Space Research  
Station) 62 p

N80-7353

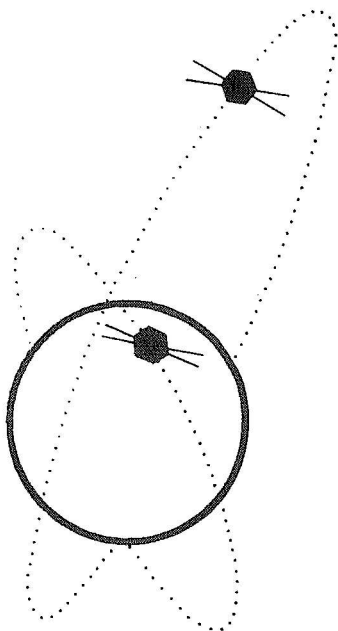
Unclas  
00/46 33644

AN ATLAS OF

# ALOUETTE-II IONOGRAMS



RECORDED AT PORT STANLEY,  
SINGAPORE AND WINKFIELD  
DURING THE FIRST MONTH  
AFTER LAUNCH.



AN ATLAS OF ALOUSTTE II IONOGRAMS  
RECORDED AT PORT STANLEY, SINGAPORE AND WINKFIELD  
DURING THE MONTH AFTER LAUNCH

Radio and Space Research Station,  
Ditton Park,  
Slough,  
England.

January, 1966

I.

CONTENTS

	<u>Page</u>
Introduction .....	II
Relevant Details of the Satellite and Data Acquisition System	II
An Outline of the Phenomena illustrated by the Ionograms in the Atlas .....	III
Captions to Plates 1 to 47 .....	V
Plates 1 to 47	

---

## II.

### Introduction

This Atlas contains plates showing topside ionograms recorded by means of the Alouette II satellite. Apart from the general outline given below of the phenomena which may be seen illustrated by the plates, the captions for the various plates contain specific comments relating to the individual ionograms and the phenomena which they illustrate.

### Relevant Details of the Satellite and Data Acquisition System

The Alouette II satellite was designed and built at the Defence Research Telecommunications Establishment in Ottawa, Canada, and launched into orbit, as part of the ISIS-X payload, on 29 November, 1965, by the United States National Aeronautics and Space Administration. The satellite is in an orbit having an apogee of 2982 km, perigee of 502 km and inclination of  $80^{\circ}$ .

Alouette II carries several experiments, but the present volume contains data from only the topside sounder which is a swept-frequency ionosonde operating over the frequency range between 0.12 Mc/s and 14.5 Mc/s. An ionogram is recorded every 30.5 seconds approximately, and the frequency sweep rate varies from about  $0.15 \text{ Mc/s}^2$  at 0.12 Mc/s to about  $0.5 \text{ Mc/s}^2$  at 2 Mc/s; above 2 Mc/s the sweep rate is approximately linear at  $1 \text{ Mc/s}^2$ .

There is no data storage facility on the spacecraft and the data are thus acquired in real time at the various data acquisition stations operated by the United States of America, Canada and the United Kingdom. The present Atlas shows ionograms recorded at the two special satellite

### III.

data acquisition stations operated by the United Kingdom Radio and Space Research Station, viz. Port Stanley ( $52^{\circ}\text{S}$ ,  $58^{\circ}\text{W}$ ) and Singapore ( $1^{\circ}\text{N}$ ,  $104^{\circ}\text{E}$ ) and also at Winkfield ( $51^{\circ}\text{N}$ ,  $1^{\circ}\text{W}$ ) which is one of the N.A.S.A. Stadan stations although it is operated by the R.S.R.S. The data recorded at these three stations are all processed to ionograms on film at the R.S.R.S., Slough.

#### An Outline of the Phenomena illustrated by the Ionograms in the Atlas

The ionograms reproduced in the present Atlas have been selected to illustrate different types of Alouette II ionogram which have been observed, and they also show various phenomena which have appeared from time-to-time on the ionograms. The plates illustrate the following:-

##### (a) Typical normal ionograms: Plates 1 to 16

Various different types of normal ionogram may be seen, many of which show different phenomena including, for example, the effects which result from the sudden change in the sounder sweep rate at 2 Mc/s. The existence of marked gradients of ionization is indicated by the fact that consecutive ionograms on particular passes are sometimes strikingly different.

##### (b) Typical oblique ionograms: Plates 17 to 21

It will be seen that traces which, at first sight, appear to have been produced by vertically reflected echoes have, in fact, been produced by oblique reflections. On several occasions it has been found impossible to decide whether the main trace was due to vertical or to oblique reflections.

#### IV.

- (c) Additional "coupled" echo traces which occur between the O-plasma resonance and the Z trace: Plates 6 and 35 to 39

Illustrations of the additional "coupled" echo traces are shown (see Plate 37 for example) and it is suggested that the "inclined resonance" phenomenon (illustrated on Plate 38) is associated with the coupled echo traces in some way.

- (d) Ducted echoes: Plates 28 to 34

Several of the plates show that, when a whole set of ducted echoes are all received at the same place, the echoes all terminate at the same frequency. Plate 33 reveals a situation in which coupling appears to have occurred between a ducted echo trace and a slightly oblique X trace.

- (e) The gradual convergence of oblique echoes: Plate 22

- (f) Spread-F traces which occur at virtual depths SMALLER than that of the main trace: Plate 23

- (g) Spread-F traces which occur at virtual depths GREATER than that of the main trace: Plate 24

- (h) Sequences showing the development of various types of spread-F echoes: Plates 25 to 27

- (i) Z traces: Plates 40 to 42

It may be seen that Z traces are frequently more complete than either the O or X traces, but that on some occasions the Z traces appear to be "broken" in the middle.

- (j) X traces with "loops": Plate 43

- (k) "Modulation" of the resonances: Plate 44

- (l) Satellite spin effects: Plates 45 to 47

Plates 45 to 47 show that the different satellite antenna orientations which exist when consecutive ionograms are recorded give rise to apparently very different consecutive ionograms.

V.

CAPTIONS TO PLATES 1-47

- Plate 1: A typical ionogram from Pass 231 over Winkfield.  
18 Dec 65, 15.56.39 U.T., 62°W, 79°N, 2811 km
- Plate 2: A typical ionogram from Pass 232 over Winkfield.  
18 Dec 65, 18.04.32 U.T., 28°W, 75°N, 2955 km
- Plate 3: A typical ionogram from Pass 38 over Winkfield.  
The Z, O and X traces can all be seen.  
2 Dec 65, 08.49.57 U.T., 7°E, 31°N, 1101 km
- Plate 4: A typical ionogram from Pass 38 over Winkfield.  
The Z, O and X traces can all be seen.  
2 Dec 65, 08.50.27 U.T., 8°E, 33°N, 1131 km
- Plate 5: A typical ionogram from Pass 38 over Winkfield.  
2 Dec 65, 08.50.58 U.T., 8°E, 34°N, 1163 km
- Plate 6: Three ionograms from Pass 38 over Winkfield. The general complexity of the "Z trace" echoes is unexpected and is due to the existence of additional "coupled" echoes which start near the base of the O-plasma resonance (at low virtual depths) and almost merge with the Z trace itself (at high virtual depths).  
The phenomena shown in this Plate should be studied in conjunction with Plates 35 to 39; Plate 37, in particular, shows a good example of the additional "coupled" echoes.  
(a) 2 Dec 65, 08.48.57 U.T., 7°E, 28°N, 1042 km  
(b) 2 Dec 65, 08.49.57 U.T., 7°E, 31°N, 1101 km  
(c) 2 Dec 65, 08.50.27 U.T., 8°E, 33°N, 1131 km
- Plate 7: A typical ionogram from Pass 14 over Winkfield.  
30 Nov 65, 08.16.13 U.T., 21°E, 37°N, 1134 km

# VI.

## Plates 8, 9, 10, 11 and 12:

Five consecutive ionograms from Pass 176 over Port Stanley. The critical frequency is almost the same on each of the ionograms, but the frequency at which the X trace starts (at zero virtual depth) varies. This means that the kinks which occur at 2 Mc/s (when the sounder sweep rate alters) fall on relatively different parts of the ionograms. Plate 11 illustrates the decrease in the trace thickness which occurs when the sweep rate alters.

Plate 8: 14 Dec 65, 01.35.39 U.T., 72°W, 61°S, 1021 km  
 Plate 9: 14 Dec 65, 01.36.09 U.T., 71°W, 63°S, 994 km  
 Plate 10: 14 Dec 65, 01.36.40 U.T., 69°W, 65°S, 996 km  
 Plate 11: 14 Dec 65, 01.37.10 U.T., 68°W, 66°S, 940 km  
 Plate 12: 14 Dec 65, 01.37.40 U.T., 66°W, 68°S, 914 km

## Plate 13:

A typical ionogram from Pass 122 over Singapore; no echoes were received between 2 and 4.5 Mc/s. It will be seen from Plates 45 to 47 that consecutive ionograms from some passes over Singapore have different frequency ranges within which no echoes are detected; this phenomenon is obviously caused by satellite spin.

9 Dec 65, 11.58.27 U.T., 123°E, 10°S, 2248 km

## Plate 14:

Two ionograms from Pass 158 over Singapore.

(a): 12 Dec 65, 12.46.28 U.T., 103°E, 4°N, 2423 km  
 (b): 12 Dec 65, 12.48.30 U.T., 104°E, 1°S, 2319 km

## Plates 15 and 16:

Twelve ionograms from Pass 232 over Winkfield. A sudden change will be noticed between ionograms (c) and (d) on Plate 16.

Plate 15(a): 18 Dec 65, 18.02.32 UT, 43°W, 78°N, 2921 km  
 (b): 18 Dec 65, 18.03.02 UT, 37°W, 77°N, 2931 km  
 (c): 18 Dec 65, 18.04.02 UT, 31°W, 76°N, 2947 km  
 (d): 18 Dec 65, 18.04.32 UT, 28°W, 75°N, 2955 km  
 (e): 18 Dec 65, 18.05.03 UT, 26°W, 74°N, 2962 km  
 (f): 18 Dec 65, 18.05.33 UT, 23°W, 73°N, 2968 km

Plate 16(a): 18 Dec 65, 18.06.03 UT, 21°W, 72°N, 2974 km  
 (b): 18 Dec 65, 18.06.33 UT, 20°W, 71°N, 2979 km  
 (c): 18 Dec 65, 18.07.33 UT, 16°W, 70°N, 2987 km  
 (d): 18 Dec 65, 18.08.03 UT, 15°W, 69°N, 2990 km  
 (e): 18 Dec 65, 18.09.15 UT, 12°W, 66°N, 2995 km  
 (f): 18 Dec 65, 18.09.45 UT, 11°W, 65°N, 2996 km

## VII.

### Plate 17:

Three ionograms from Pass 173 over Winkfield. Ionogram (a) shows two traces which at first sight appear to be the normal O and X traces. Ionograms (b) and (c), however, show a third trace which suggests that at least one of the other two traces must be produced by oblique reflections.

- (a) 13 Dec 65, 18.52.15 U.T.,  $1^{\circ}\text{E}$ ,  $42^{\circ}\text{N}$ , 2944 km
- (b) 13 Dec 65, 18.53.15 U.T.,  $1^{\circ}\text{E}$ ,  $40^{\circ}\text{N}$ , 2928 km
- (c) 13 Dec 65, 18.54.46 U.T.,  $2^{\circ}\text{E}$ ,  $37^{\circ}\text{N}$ , 2898 km

### Plate 18:

Four ionograms from Pass 146 over Singapore. Ionogram (c) shows a single trace which at first sight may be assumed to be a normal X trace. A study of the other ionograms shows, however, that the single trace on ionogram (c) was produced by oblique reflections.

- (a) 11 Dec 65, 12.33.02 U.T.,  $110^{\circ}\text{E}$ ,  $7^{\circ}\text{S}$ , 2229 km
- (b) 11 Dec 65, 12.33.32 U.T.,  $110^{\circ}\text{E}$ ,  $8^{\circ}\text{S}$ , 2201 km
- (c) 11 Dec 65, 12.34.02 U.T.,  $111^{\circ}\text{E}$ ,  $10^{\circ}\text{S}$ , 2173 km
- (d) 11 Dec 65, 12.35.02 U.T.,  $111^{\circ}\text{E}$ ,  $12^{\circ}\text{S}$ , 2116 km

### Plate 19:

A typical ionogram from Pass 227 over Winkfield. It is impossible to decide whether or not the X trace was produced by oblique reflections.

18 Dec 65, 07.37.54 U.T.,  $5^{\circ}\text{E}$ ,  $55^{\circ}\text{N}$ , 2236 km

### Plate 20:

A typical ionogram from Pass 274 over Winkfield. It is impossible to decide whether or not the X trace was produced by oblique reflections.

22 Dec 65, 06.46.06 U.T.,  $9^{\circ}\text{E}$ ,  $50^{\circ}\text{N}$ , 2296 km

### Plate 21:

Two ionograms from Passes (a) 101 over Winkfield and (b) 113 over Winkfield respectively. It is impossible to decide whether or not the X trace was produced by oblique reflections.

- (a) 7 Dec 65, 16.57.24 U.T.,  $34^{\circ}\text{E}$ ,  $57^{\circ}\text{N}$ , 2950 km
- (b) 8 Dec 65, 17.14.00 U.T.,  $26^{\circ}\text{E}$ ,  $60^{\circ}\text{N}$ , 2942 km

# VIII.

## Plate 22:

Six ionograms from Pass 3 over Winkfield. The series of ionograms shows the gradual convergence of the normal and oblique sets of traces.

- (a) 29 Nov 65, 10.07.13 U.T., 4°E, 59°N, 1566 km
- (b) 29 Nov 65, 10.08.16 U.T., 7°E, 62°N, 1632 km
- (c) 29 Nov 65, 10.08.48 U.T., 8°E, 64°N, 1669 km
- (d) 29 Nov 65, 10.10.22 U.T., 12°E, 68°N, 1771 km
- (e) 29 Nov 65, 10.11.26 U.T., 16°E, 71°N, 1840 km
- (f) 29 Nov 65, 10.11.58 U.T., 19°E, 72°N, 1873 km

## Plate 23:

Two ionograms from Pass 168 over Winkfield. Both ionograms show additional "spread-F" traces which all occur at virtual depths smaller than that of the main X trace.

- (a) 13 Dec 65, 08.05.58 U.T., 2°E, 43°N, 1766 km
- (b) 13 Dec 65, 08.06.28 U.T., 3°E, 44°N, 1798 km

## Plate 24:

Two ionograms from Pass 73 over Winkfield. Ionogram (b) shows a set of additional traces which all occur at virtual depths greater than that of the main X trace.

- (a) 5 Dec 65, 07.42.57 U.T., 20°E, 36°N, 1288 km
- (b) 5 Dec 65, 07.44.27 U.T., 21°E, 40°N, 1384 km

## Plate 25:

Six ionograms from Pass 28 over Singapore. The spread-F seems to consist of additional traces which occur between the main X trace (clearly visible on ionograms (a) and (f)) and a pronounced oblique trace (clearly visible on ionograms (b) and (d)).

- (a) 1 Dec 65, 13.45.45 U.T., 114°E, 29°S, 2167 km
- (b) 1 Dec 65, 13.44.44 U.T., 114°E, 26°S, 2223 km
- (c) 1 Dec 65, 13.44.14 U.T., 114°E, 25°S, 2251 km
- (d) 1 Dec 65, 13.43.11 U.T., 113°E, 22°S, 2308 km
- (e) 1 Dec 65, 13.42.42 U.T., 113°E, 21°S, 2333 km
- (f) 1 Dec 65, 13.42.10 U.T., 113°E, 20°S, 2361 km

## Plate 26:

An ionogram from Pass 109 over Winkfield. The traces comprising the spread-F echoes are similar to that shown in ionogram (e) of Plate 25.

- 8 Dec 65, 08.36.27 U.T., 1°E, 37°N, 1422 km

## IX.

### Plate 27:

Four ionograms from Pass 200 over Singapore. The ionograms show different stages in the development of an important set of oblique echoes.

- (a) 16 Dec 65, 00.37.53 U.T.,  $99^{\circ}\text{E}$ ,  $6^{\circ}\text{S}$ , 912 km
- (b) 16 Dec 65, 00.38.23 U.T.,  $99^{\circ}\text{E}$ ,  $4^{\circ}\text{S}$ , 939 km
- (c) 16 Dec 65, 00.39.54 U.T.,  $99^{\circ}\text{E}$ ,  $1^{\circ}\text{N}$ , 1022 km
- (d) 16 Dec 65, 00.40.25 U.T.,  $100^{\circ}\text{E}$ ,  $3^{\circ}\text{N}$ , 1052 km

### Plate 28:

Two ionograms from Passes (a) 52 over Singapore and (b) 40 over Singapore respectively. The ionograms show traces which appear to have been reflected at small virtual depths, but which have actually been reflected at such large virtual depths that they have been received back in the receiver during the sweep associated with the succeeding transmitted pulse.

- (a) 3 Dec 65, 14.01.24 U.T.,  $98^{\circ}\text{E}$ ,  $19^{\circ}\text{N}$ , 2908 km
- (b) 2 Dec 65, 13.45.26 U.T.,  $104^{\circ}\text{E}$ ,  $15^{\circ}\text{N}$ , 2883 km

### Plate 29:

An ionogram from Pass 99 over Singapore. The ionogram shows a typical example of ducted echoes; it should be noted that all the ducted echo traces terminate at the same frequency.

7 Dec 65, 13.23.27 U.T.,  $105^{\circ}\text{E}$ ,  $8^{\circ}\text{S}$ , 2363 km

### Plate 30:

An ionogram from Pass 52 over Singapore. The ionogram shows a typical example of a ducted echo pattern.

3 Dec 65, 14.04.54 U.T.,  $98^{\circ}\text{E}$ ,  $11^{\circ}\text{S}$ , 2824 km

### Plate 31:

An ionogram from Pass 173 over Winkfield. The ionogram shows a group of three traces formed by strong ducted echoes.

13 Dec 65, 18.58.18 U.T.,  $3^{\circ}\text{E}$ ,  $29^{\circ}\text{N}$ , 2806 km

### Plate 32:

An ionogram from Pass 344 over Winkfield. The ionogram shows strong ducted echoes which all terminate at the same frequency.

28 Dec 65, 04.22.07 U.T.,  $28^{\circ}\text{E}$ ,  $29^{\circ}\text{N}$ , 2070 km

X.

Plate 33:

An ionogram from Pass 173 over Winkfield. The traces reveal a situation in which coupling appears to have occurred between a ducted echo trace and a slightly oblique X trace.

13 Dec 65, 18.52.15 U.T.,  $1^{\circ}\text{E}$ ,  $42^{\circ}\text{N}$ , 2944 km

Plate 34:

Four ionograms from Pass 170 over Singapore. The ionograms show changes between the ducted echo pattern observed at slightly different latitudes during a pass.

- (a) 13 Dec 65, 12.52.52 U.T.,  $94^{\circ}\text{E}$ ,  $31^{\circ}\text{N}$ , 2839 km
- (b) 13 Dec 65, 12.53.22 U.T.,  $94^{\circ}\text{E}$ ,  $30^{\circ}\text{N}$ , 2825 km
- (c) 13 Dec 65, 12.54.22 U.T.,  $95^{\circ}\text{E}$ ,  $28^{\circ}\text{N}$ , 2796 km
- (d) 13 Dec 65, 12.54.52 U.T.,  $95^{\circ}\text{E}$ ,  $26^{\circ}\text{N}$ , 2780 km

Plates 35 and 36:

Two ionograms from Pass 188 over Singapore. Both ionograms show typical (rather than excellent) examples of the additional "coupled" echo traces which start at the O-plasma resonance, but which ultimately become close to and parallel with the normal Z trace. A better example of these additional traces is shown in Plate 37, and it is interesting to study these Plates in conjunction with Plates 38 and 39.

Plate 35: 15 Dec 65, 00.23.09 U.T.,  $106^{\circ}\text{E}$ ,  $4^{\circ}\text{N}$ , 1040 km

Plate 36: 15 Dec 65, 00.22.09 U.T.,  $106^{\circ}\text{E}$ ,  $1^{\circ}\text{N}$ , 987 km

Plate 37:

An ionogram from Pass 38 over Winkfield. Three additional "coupled" echo traces which emerge from the O-plasma resonance (at low virtual depths), but which eventually become close to and parallel with the normal Z trace (at larger virtual depths) may be seen.

Readers may find that the additional traces shown on the Alouette II ionograms are more easily visible if the print is held up in a horizontal position in front of them such that their eyes are almost in the plane of the ionogram.

2 Dec 65, 08.49.57 U.T.,  $7^{\circ}\text{W}$ ,  $31^{\circ}\text{N}$ , 1101 km

## XI.

- Plates 38 and 39: An ionogram from Pass 38 over Winkfield; both Plates show the same ionogram processed with different virtual height ranges. It appears, from Plate 38 particularly, that there is a single resonance associated with both the O-plasma and Z-infinity conditions, and that this resonance is inclined to the vertical axis. This phenomenon should be studied in conjunction with Plates 6 and 37; it seems reasonable to suggest that the "inclined resonance" phenomenon is associated in some way with the additional "coupled" echo traces.  
2 Dec 65, 08.52.29 U.T., 9°E, 39°N, 1258 km
- Plates 40 and 41: These Plates show five examples of almost complete Z traces (each having a typical "S-bend") while none of the other normal traces shown are complete.  
Plate 40(a): 13 Dec 65, 13.13.31 UT, 99°E, 20°S, 1860 km  
(b): 3 Dec 65, 14.16.30 UT, 100°E, 16°S, 2356 km  
(c): 3 Dec 65, 14.17.00 UT, 100°E, 17°S, 2334 km  
Plate 41(a): 13 Dec 65, 08.03.57 UT, 1°E, 37°N, 1635 km  
(b): 13 Dec 65, 08.04.27 UT, 1°E, 39°N, 1667 km
- Plate 42: Two ionograms from Passes (a) 168 over Winkfield and (b) 14 over Winkfield respectively. Both ionograms show a Z trace which appears to be "broken" in the middle.  
(a) 13 Dec 65, 08.03.26 U.T., 1°E, 36°N, 1601 km  
(b) 30 Nov 65, 08.16.44 U.T., 21°E, 38°N, 1168 km
- Plate 43: Two ionograms from Passes (a) 52 over Singapore and (b) 158 over Singapore respectively. Both ionograms show an X trace with a "loop" on it.  
(a) 3 Dec 65, 14.07.57 U.T., 99°E, 4°N, 2728 km  
(b) 12 Dec 65, 12.42.27 U.T., 102°E, 14°N, 2607 km
- Plate 44: Two ionograms from Pass 52 over Singapore. Both ionograms show a deeply modulated resonance near 0.6 Mc/s.  
(a) 3 Dec 65, 14.06.54 U.T., 98°E, 7°N, 2763 km  
(b) 3 Dec 65, 14.07.24 U.T., 99°E, 6°N, 2747 km

# XII.

## Plates 45, 46 and 47:

Seventeen consecutive ionograms from each of Passes 87 and 110 over Singapore. Each Plate contains ionograms from Pass 87 in the left-hand column and from Pass 110 in the right-hand column. Plate 45 contains the first six from each Pass, Plate 46 contains the second six and Plate 47 contains the remaining five of the seventeen ionograms.

It is immediately obvious that, for any of the seventeen pairs of corresponding ionograms, both the ionograms look alike. The ranges of frequency for which echoes were received or not received are similar for both ionograms in any particular pair.

It will also be noticed that for both Passes the echo pattern is repeated every four ionograms; for example, the first, fifth, ninth, thirteenth and seventeenth ionograms in each Pass are all similar. Obviously, the explanation of the phenomena illustrated in these Plates must involve satellite spin. The various satellite antenna orientations which exist when consecutive ionograms are recorded depend on (1) the satellite spin period and (2) the time interval between individual ionograms, and will give rise to the kind of results observed.

Plate 45(a): 6 Dec 65, 12.59.24 UT, 110°E, 6°N, 2674 km  
 (b): 6 Dec 65, 12.59.54 UT, 110°E, 5°N, 2655 km  
 (c): 6 Dec 65, 13.00.24 UT, 110°E, 4°N, 2635 km  
 (d): 6 Dec 65, 13.00.54 UT, 110°E, 3°N, 2615 km  
 (e): 6 Dec 65, 13.01.25 UT, 110°E, 2°N, 2593 km  
 (f): 6 Dec 65, 13.01.55 UT, 111°E, 1°N, 2572 km  
 (g): 8 Dec 65, 11.34.28 UT, 128°E, 5°N, 2584 km  
 (h): 8 Dec 65, 11.34.58 UT, 128°E, 4°N, 2562 km  
 (i): 8 Dec 65, 11.35.29 UT, 128°E, 2°N, 2539 km  
 (j): 8 Dec 65, 11.35.59 UT, 128°E, 1°N, 2517 km  
 (k): 8 Dec 65, 11.36.30 UT, 129°E, 0°N, 2493 km  
 (l): 8 Dec 65, 11.37.00 UT, 129°E, 1°S, 2470 km

Plate 46(a): 6 Dec 65, 13.02.25 UT, 111°E, 1°S, 2550 km  
 (b): 6 Dec 65, 13.02.55 UT, 111°E, 2°S, 2528 km  
 (c): 6 Dec 65, 13.03.26 UT, 111°E, 3°S, 2504 km  
 (d): 6 Dec 65, 13.03.56 UT, 111°E, 4°S, 2481 km  
 (e): 6 Dec 65, 13.04.26 UT, 111°E, 6°S, 2457 km  
 (f): 6 Dec 65, 13.04.56 UT, 111°E, 7°S, 2433 km  
 (g): 8 Dec 65, 11.37.30 UT, 129°E, 2°S, 2445 km  
 (h): 8 Dec 65, 11.38.00 UT, 129°E, 4°S, 2421 km  
 (i): 8 Dec 65, 11.38.30 UT, 129°E, 5°S, 2396 km  
 (j): 8 Dec 65, 11.39.00 UT, 129°E, 6°S, 2371 km  
 (k): 8 Dec 65, 11.39.31 UT, 129°E, 8°S, 2344 km  
 (l): 8 Dec 65, 11.40.01 UT, 129°E, 9°S, 2318 km

# XIII.

Plate 47 (a): 6 Dec 65, 13.05.26 UT, 111°E, 8°S, 2408 km  
 (b): 6 Dec 65, 13.05.56 UT, 111°E, 9°S, 2383 km  
 (c): 6 Dec 65, 13.06.27 UT, 111°E, 11°S, 2356 km  
 (d): 6 Dec 65, 13.06.57 UT, 112°E, 12°S, 2331 km  
 (e): 6 Dec 65, 13.07.27 UT, 112°E, 13°S, 2304 km  
 (f): 8 Dec 65, 11.40.32 UT, 129°E, 10°S, 2290 km  
 (g): 8 Dec 65, 11.41.02 UT, 130°E, 11°S, 2264 km  
 (h): 8 Dec 65, 11.41.32 UT, 130°E, 13°S, 2236 km  
 (i): 8 Dec 65, 11.42.02 UT, 130°E, 14°S, 2208 km  
 (j): 8 Dec 65, 11.42.33 UT, 130°E, 15°S, 2179 km

---

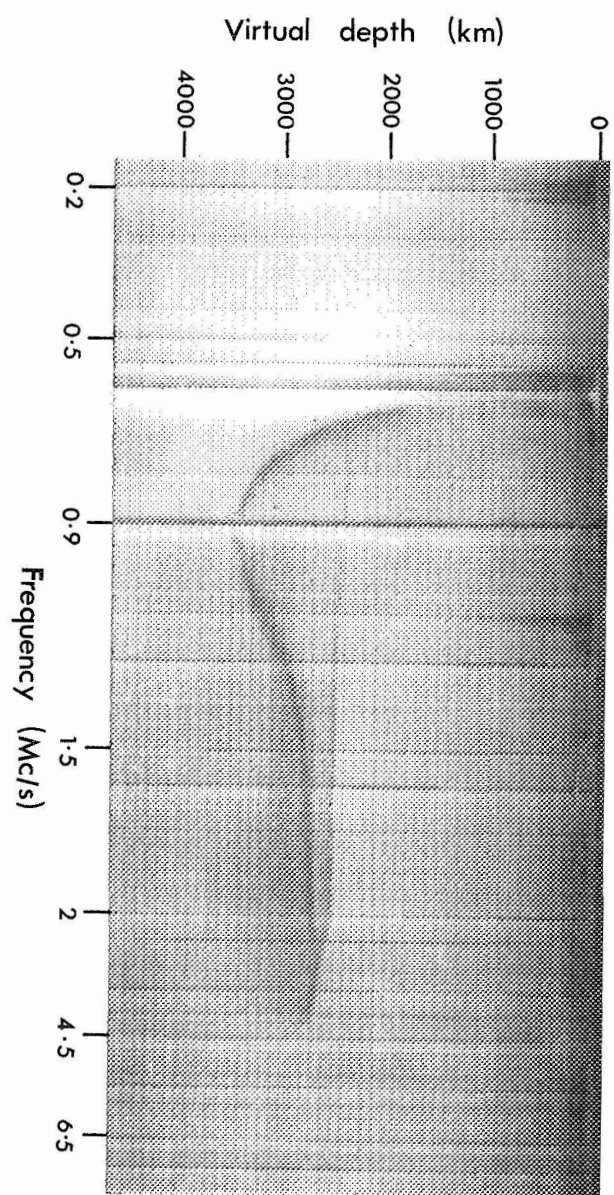


PLATE No: 1

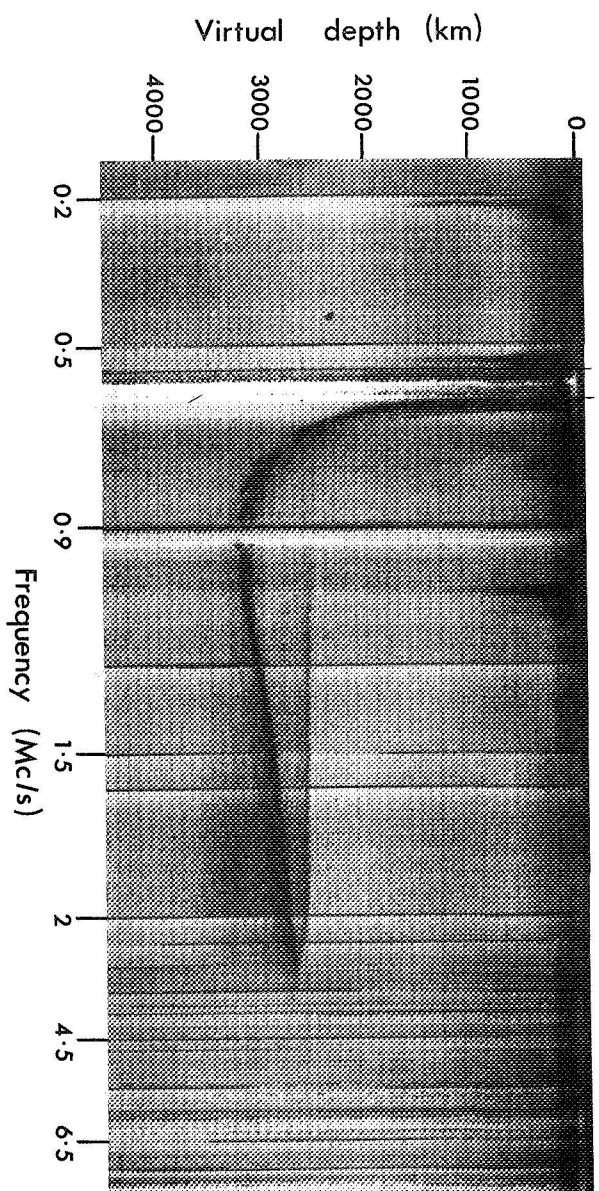


PLATE No: 2

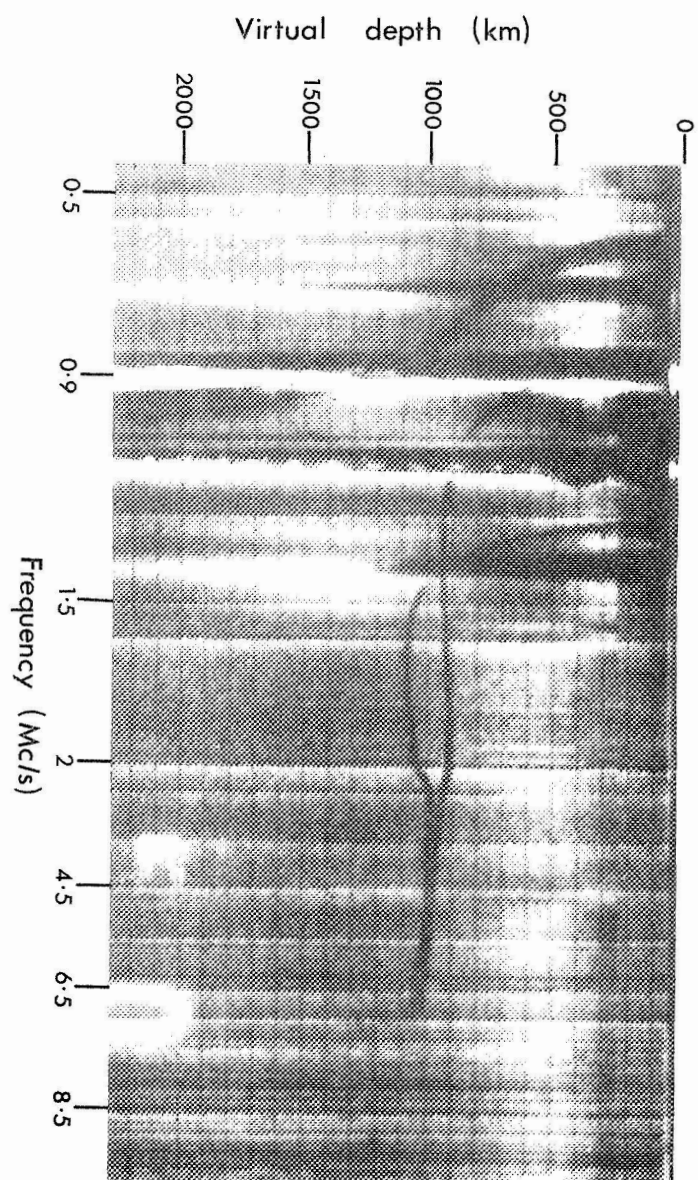


PLATE No: 3

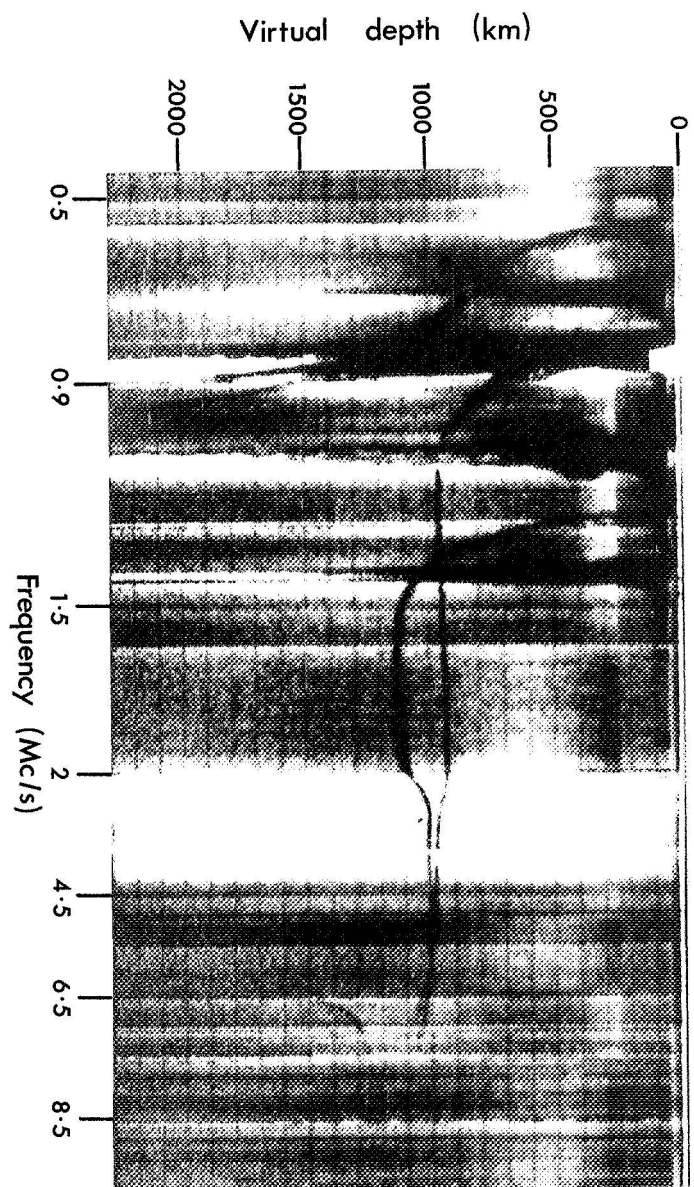


PLATE No: 4

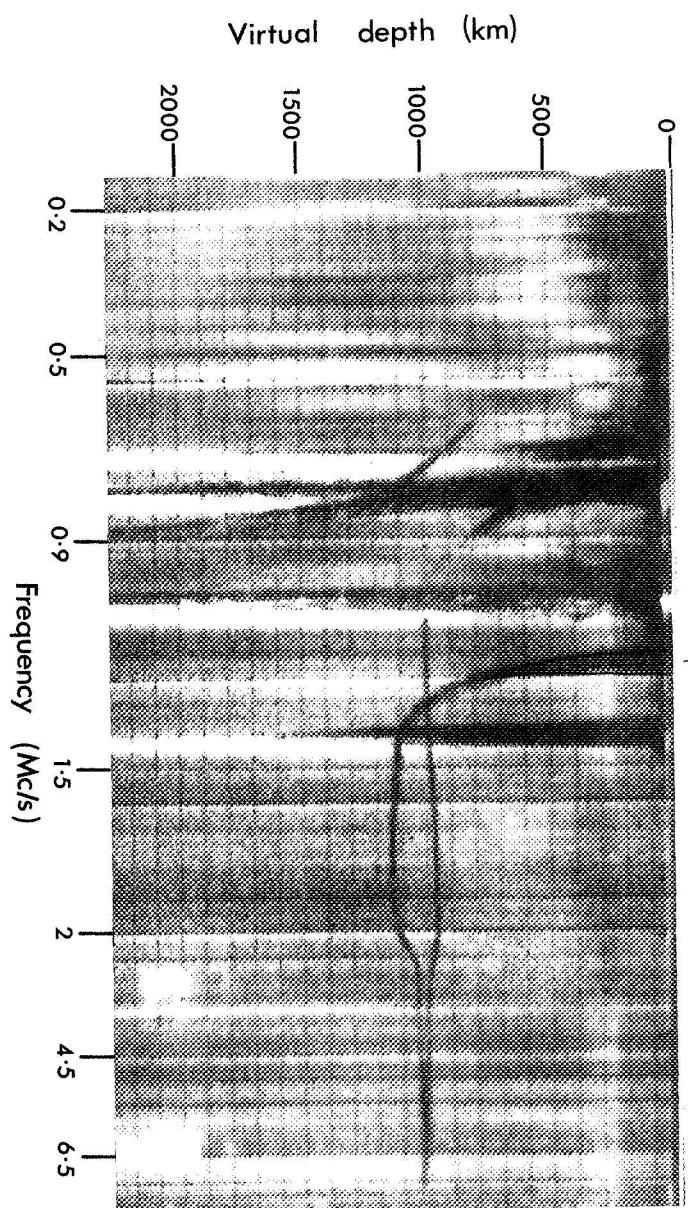


PLATE No:5

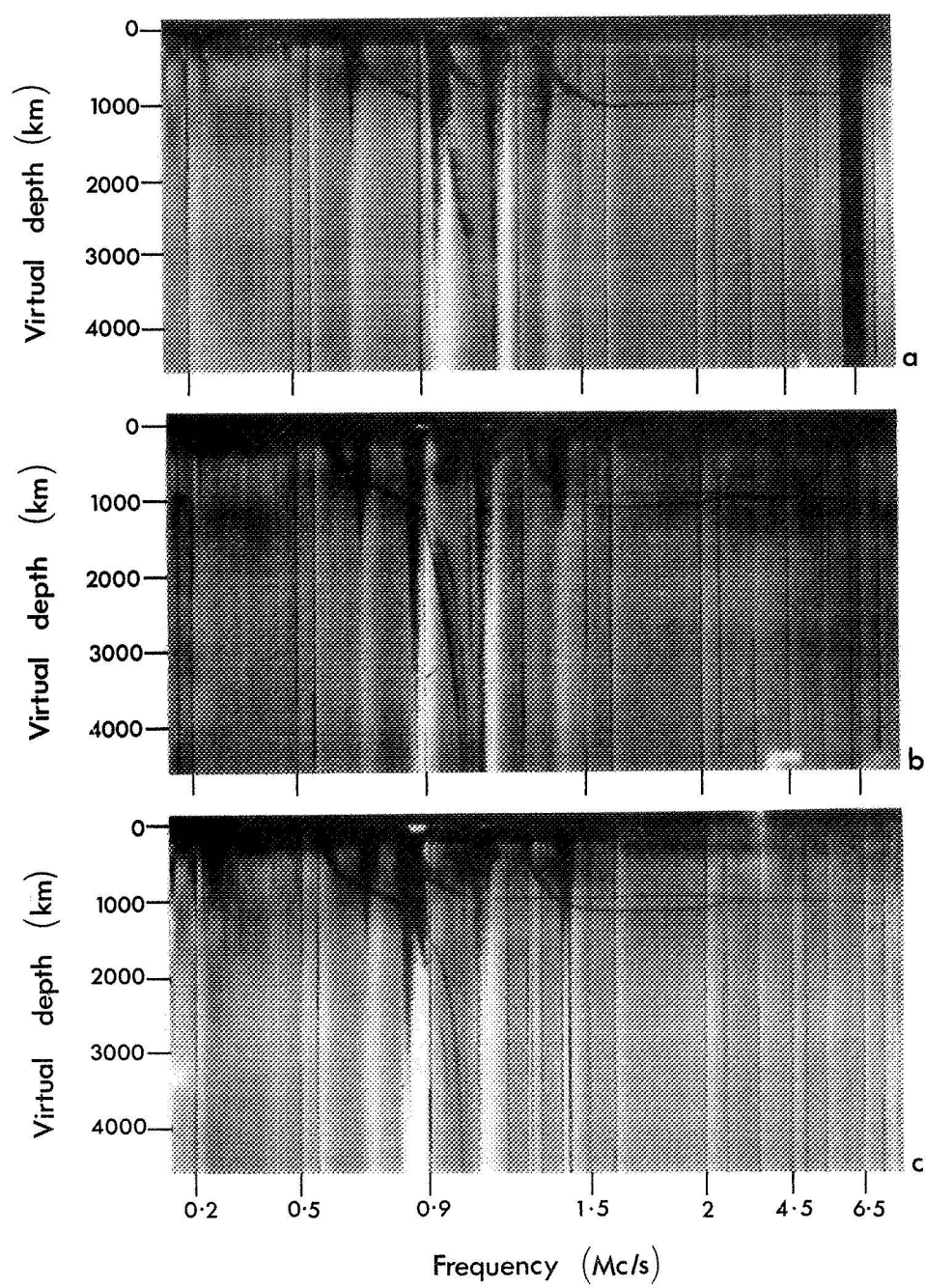


PLATE No: 6

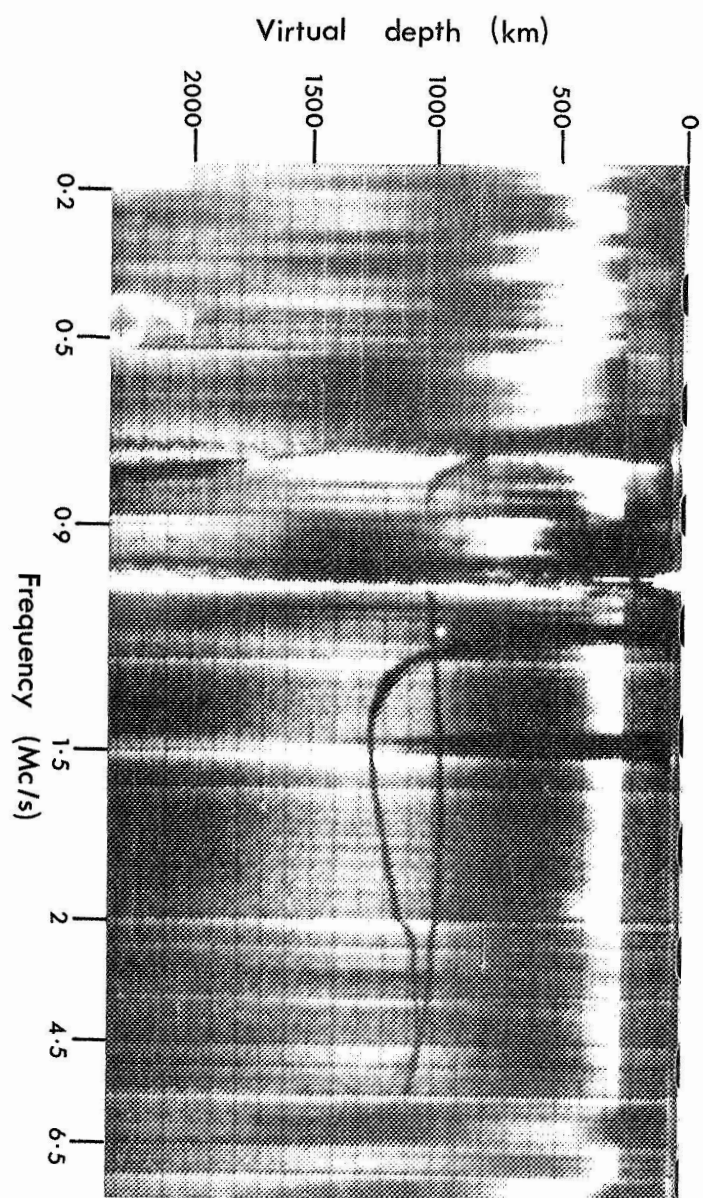


PLATE No: 7

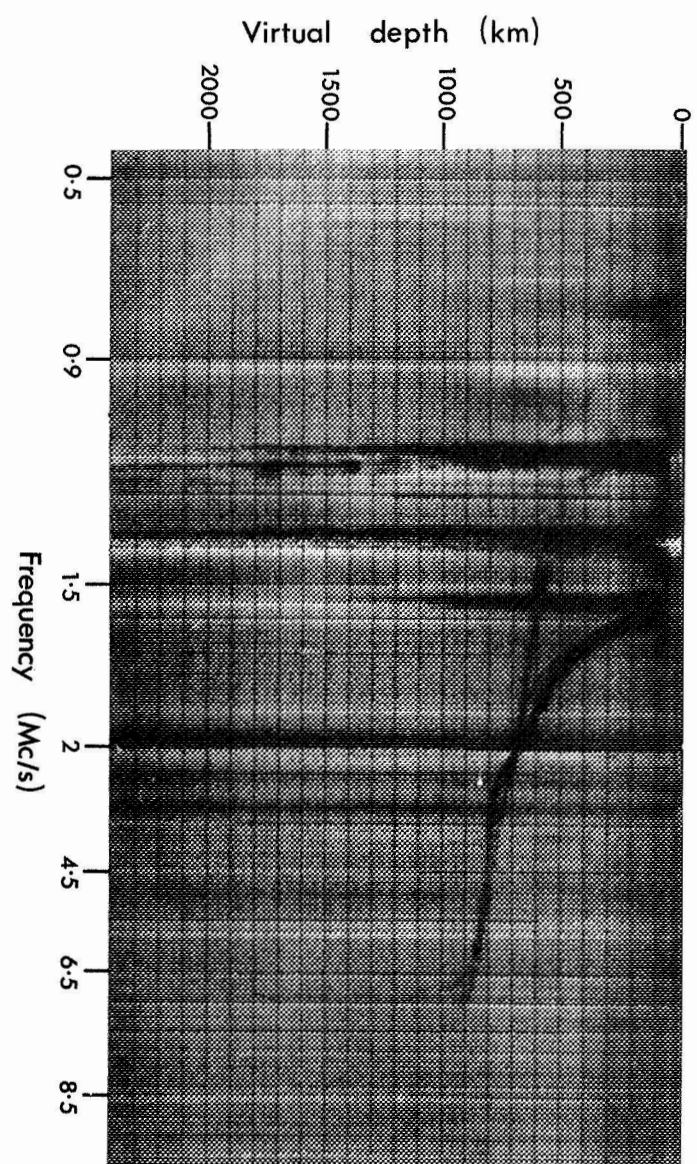


PLATE No: 8

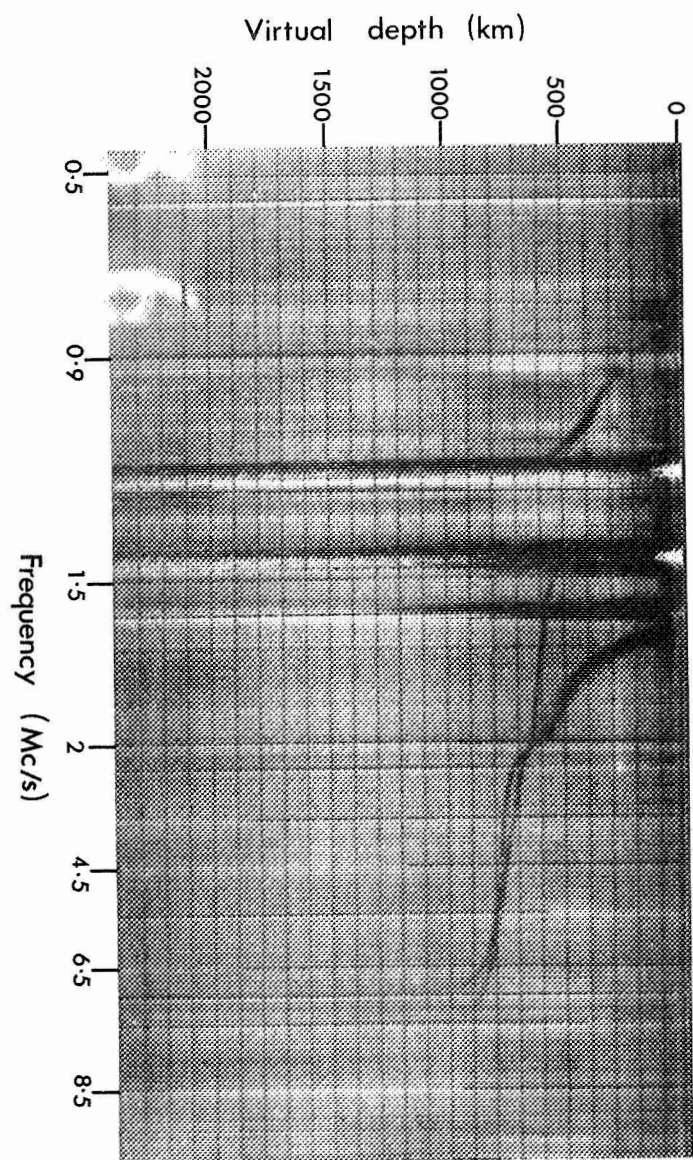


PLATE No: 9



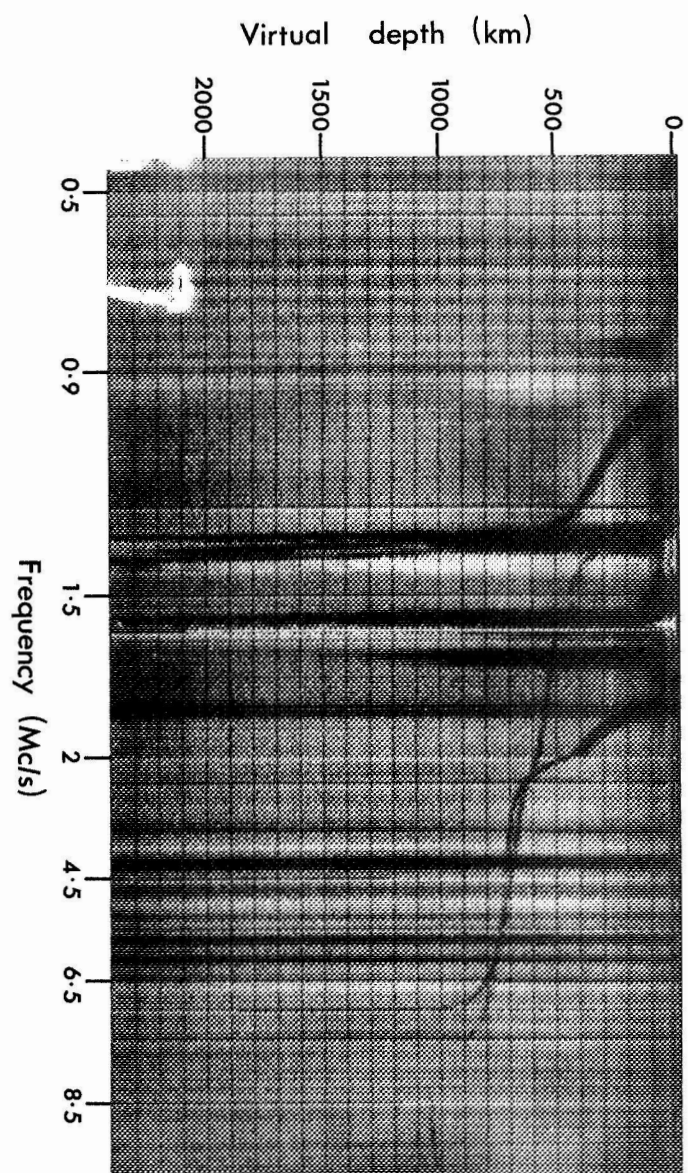


PLATE No: 11

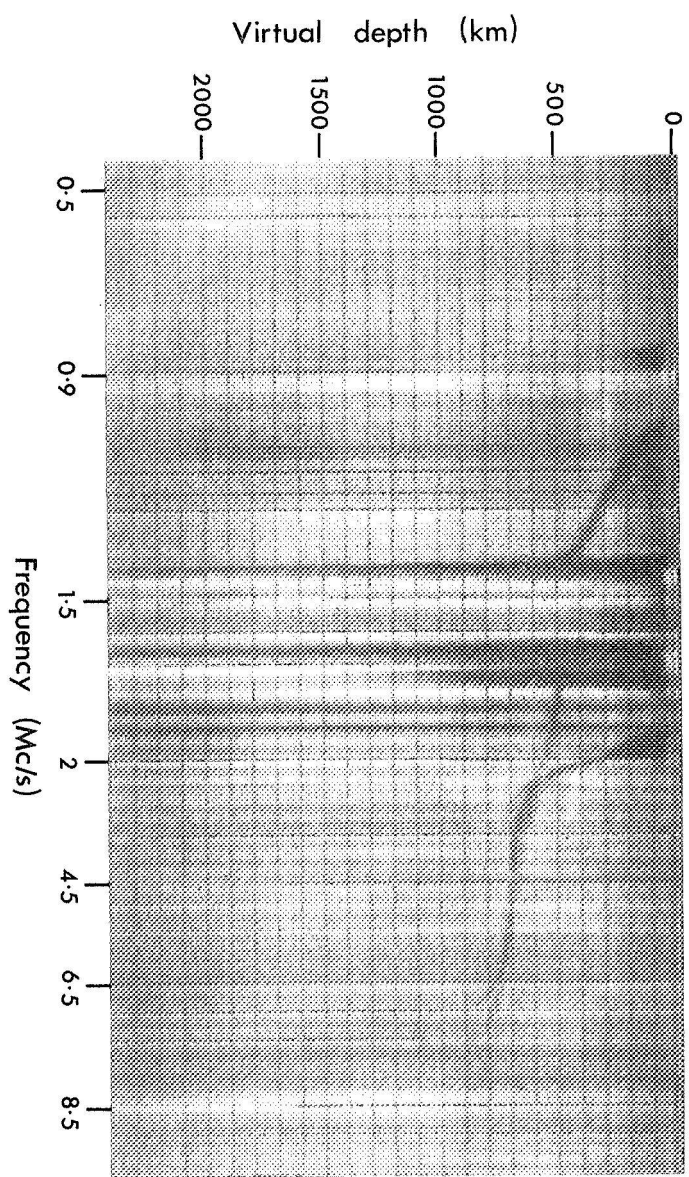


PLATE No: 12

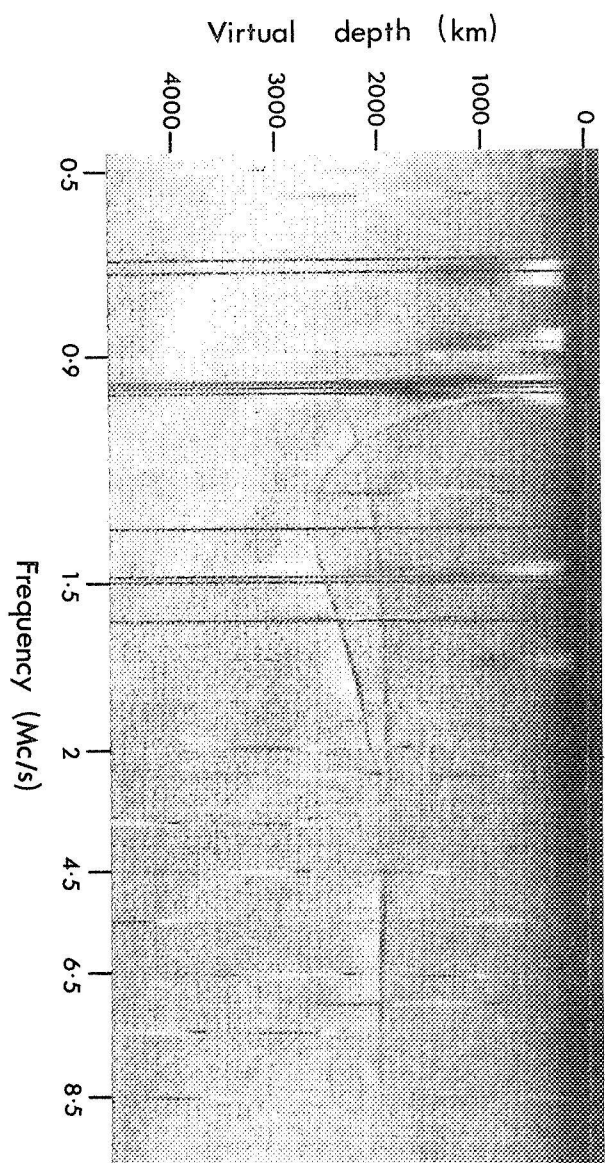


PLATE No: 13

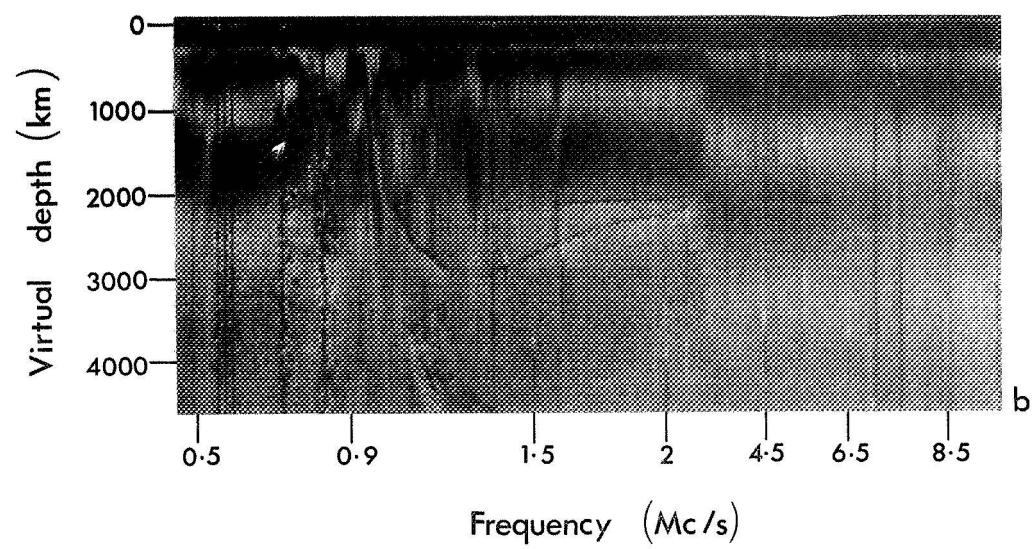
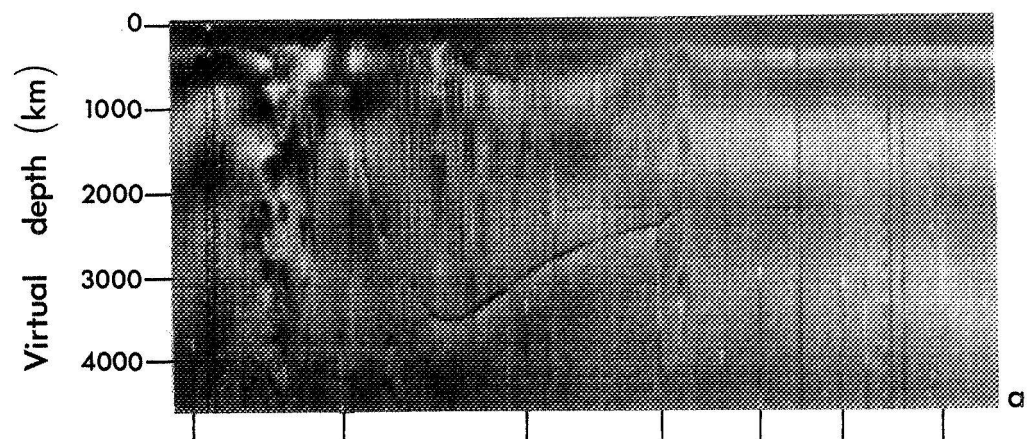


PLATE No: 14

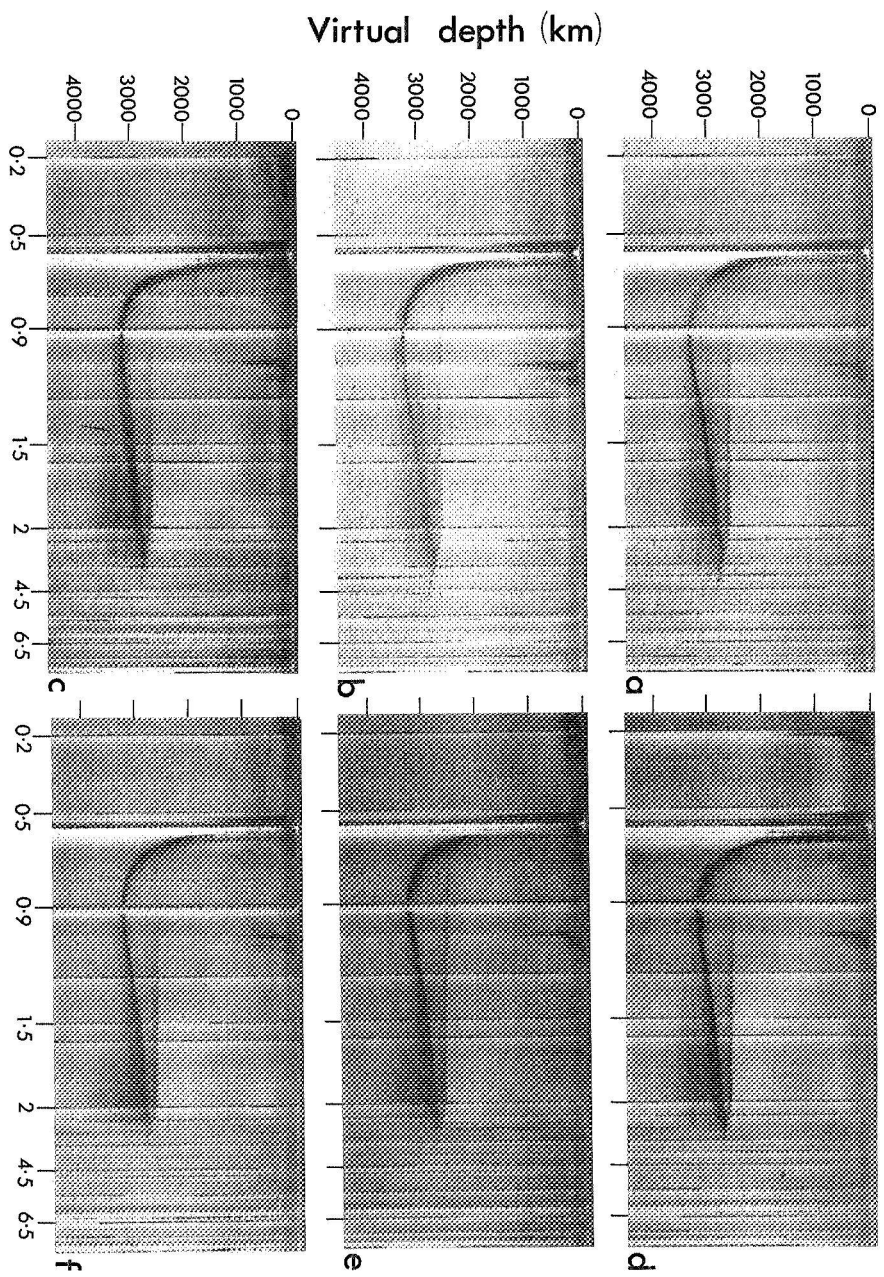


PLATE No: 15

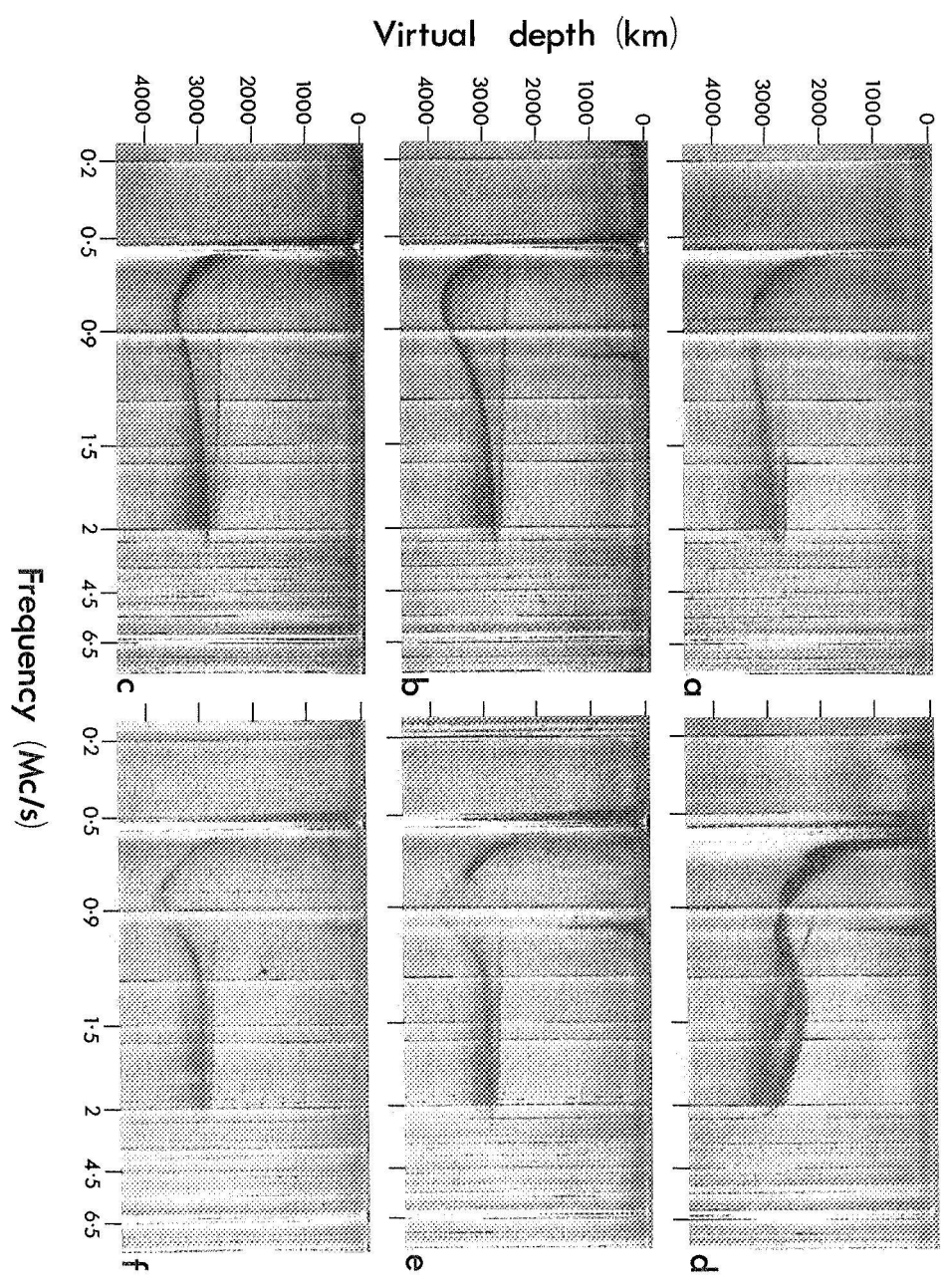


PLATE No: 16

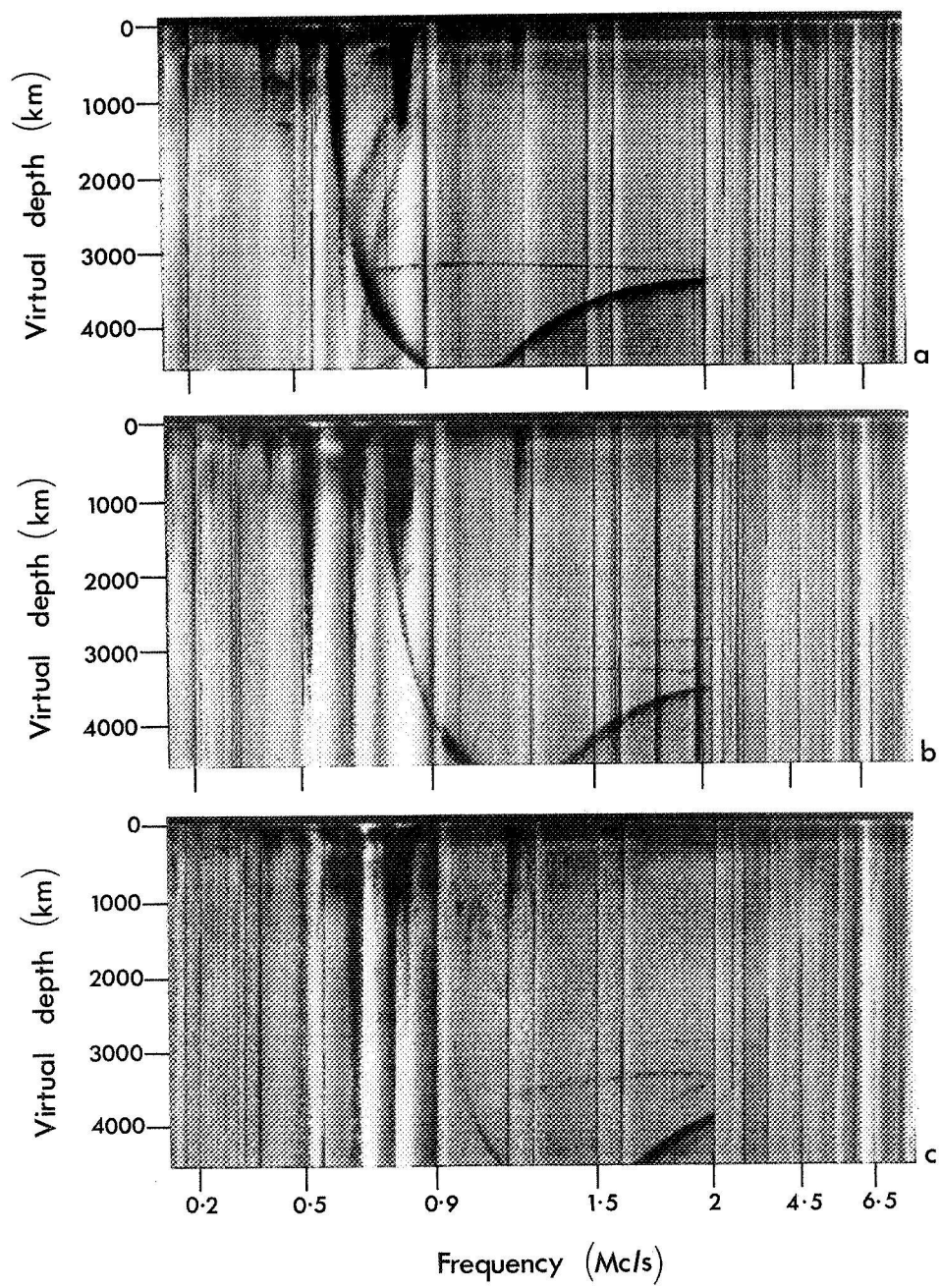


PLATE No:17

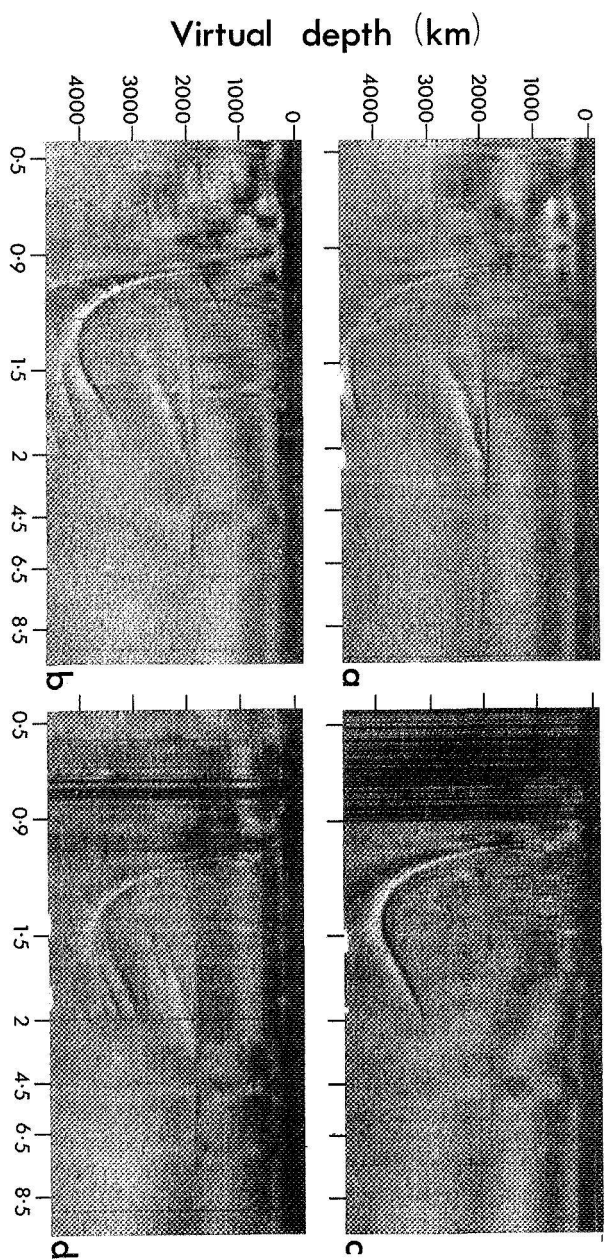


PLATE No: 18

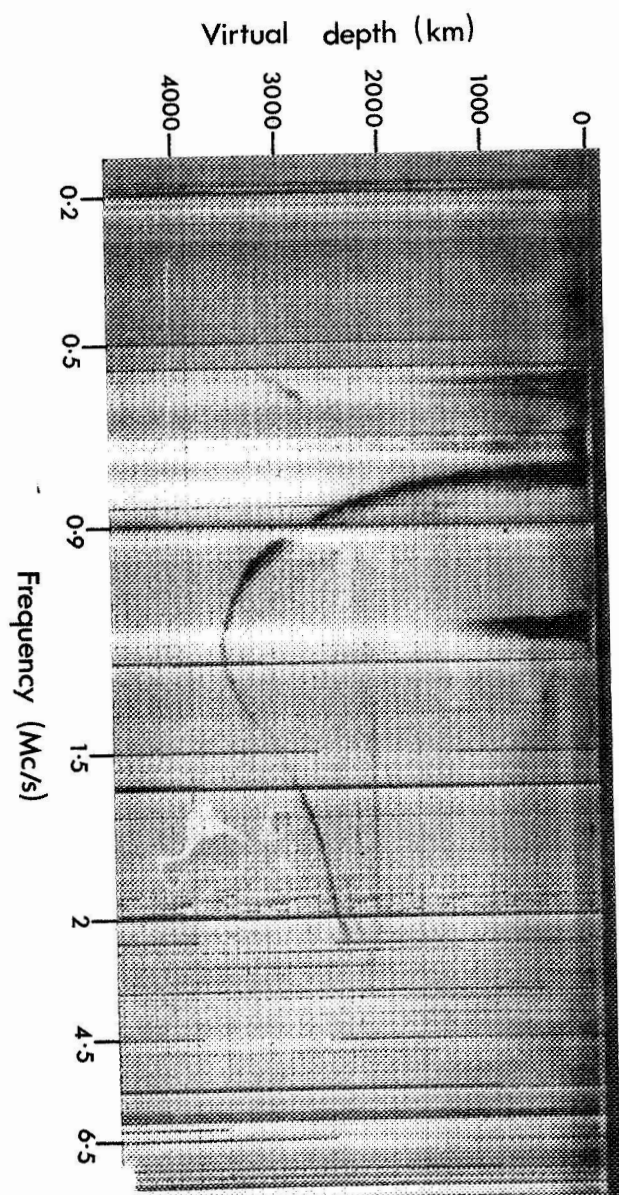


PLATE No: 19

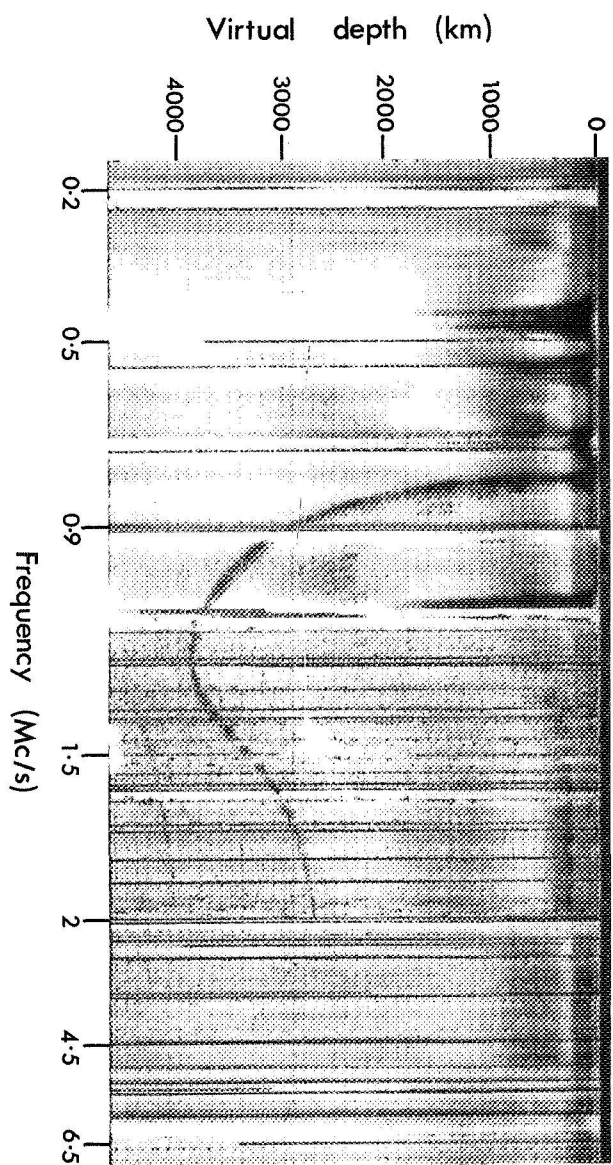


PLATE No: 20

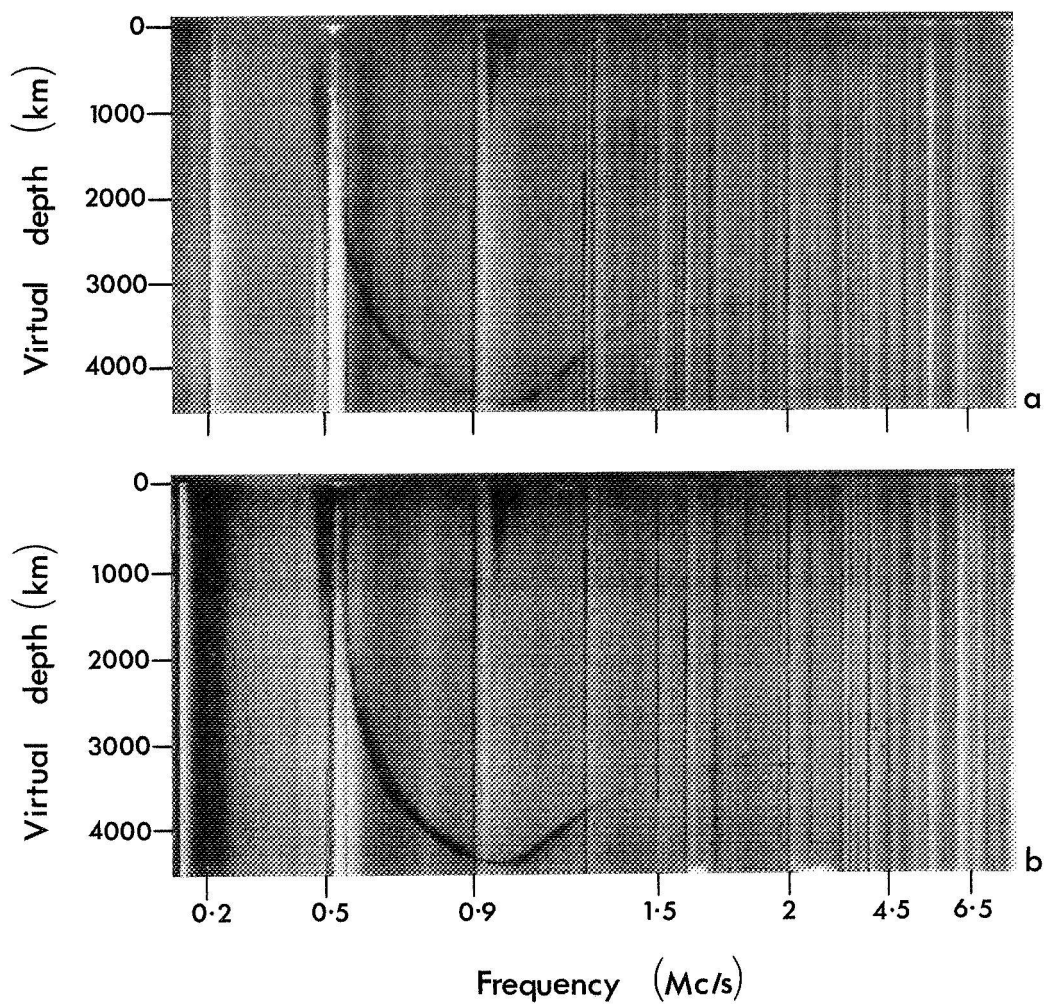


PLATE No: 21

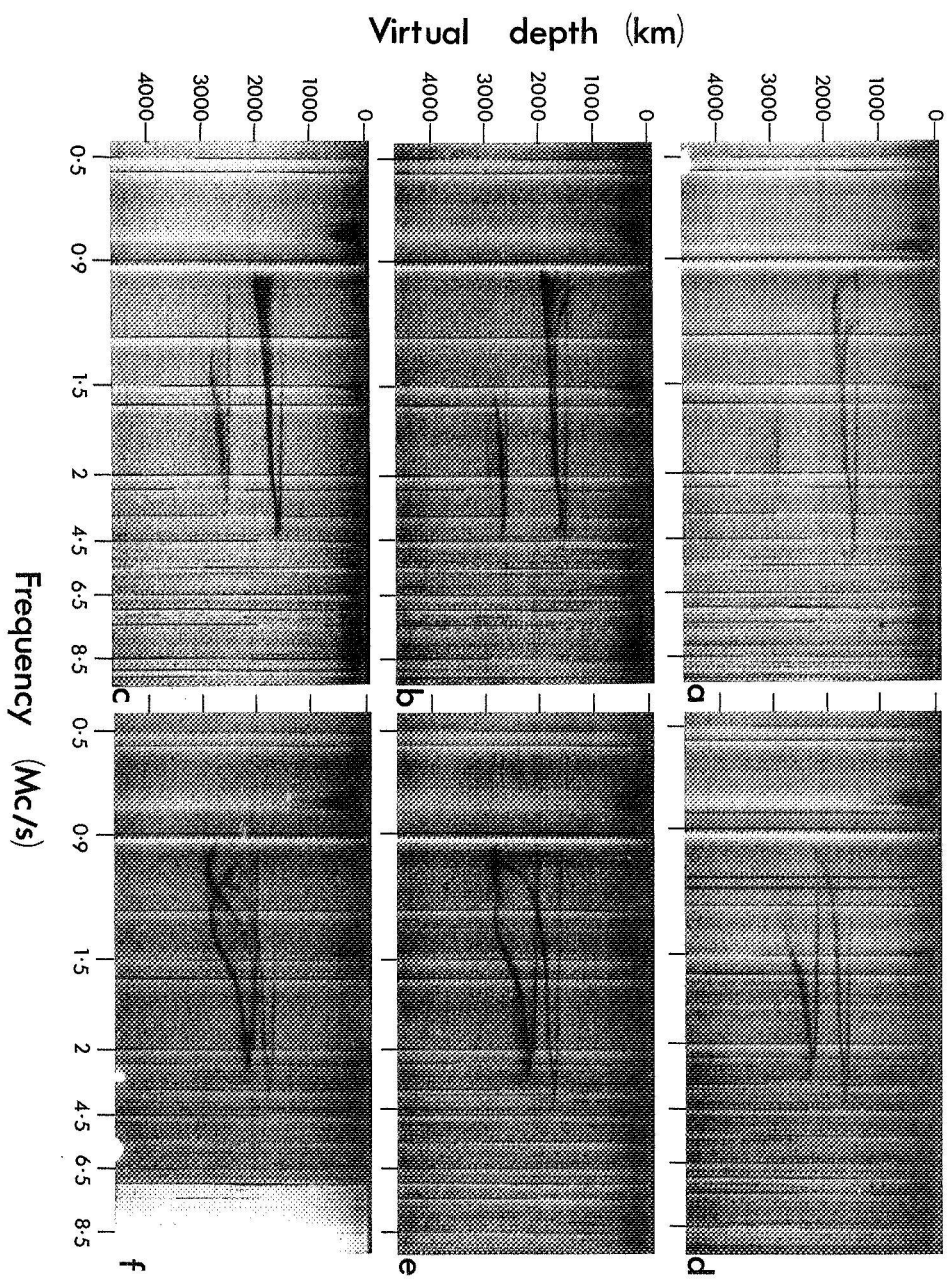


PLATE No:22

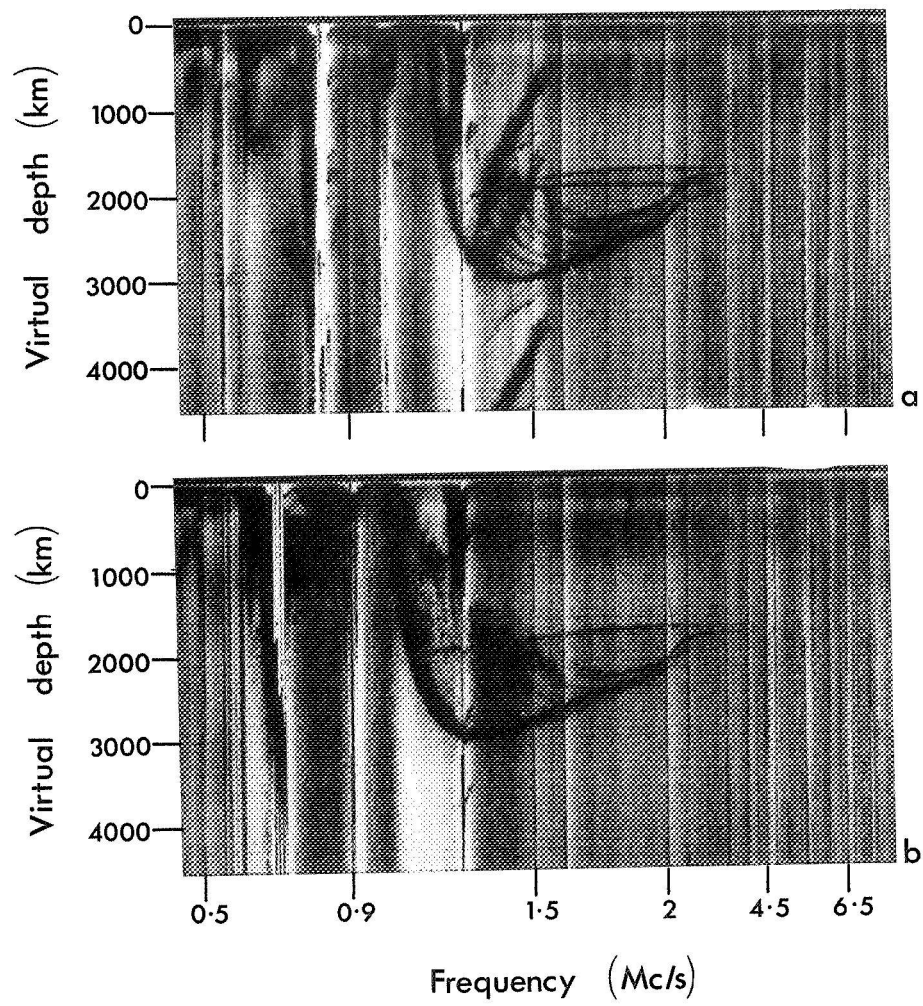


PLATE No: 23

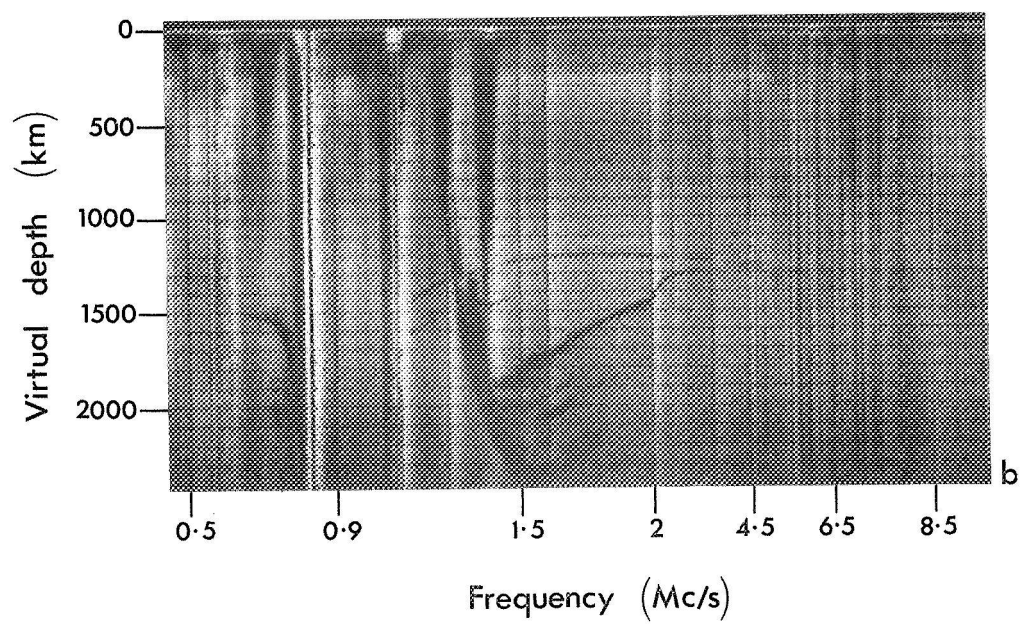
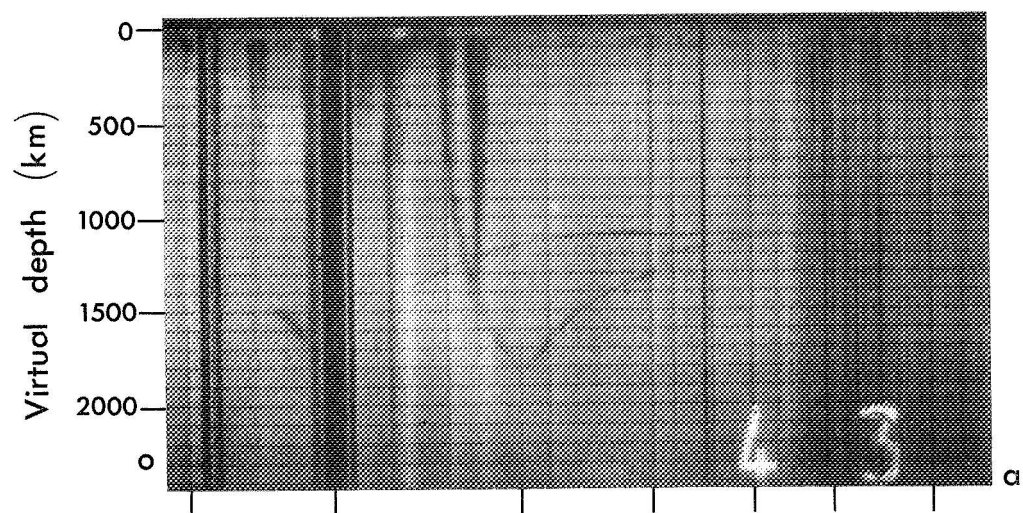


PLATE No: 24

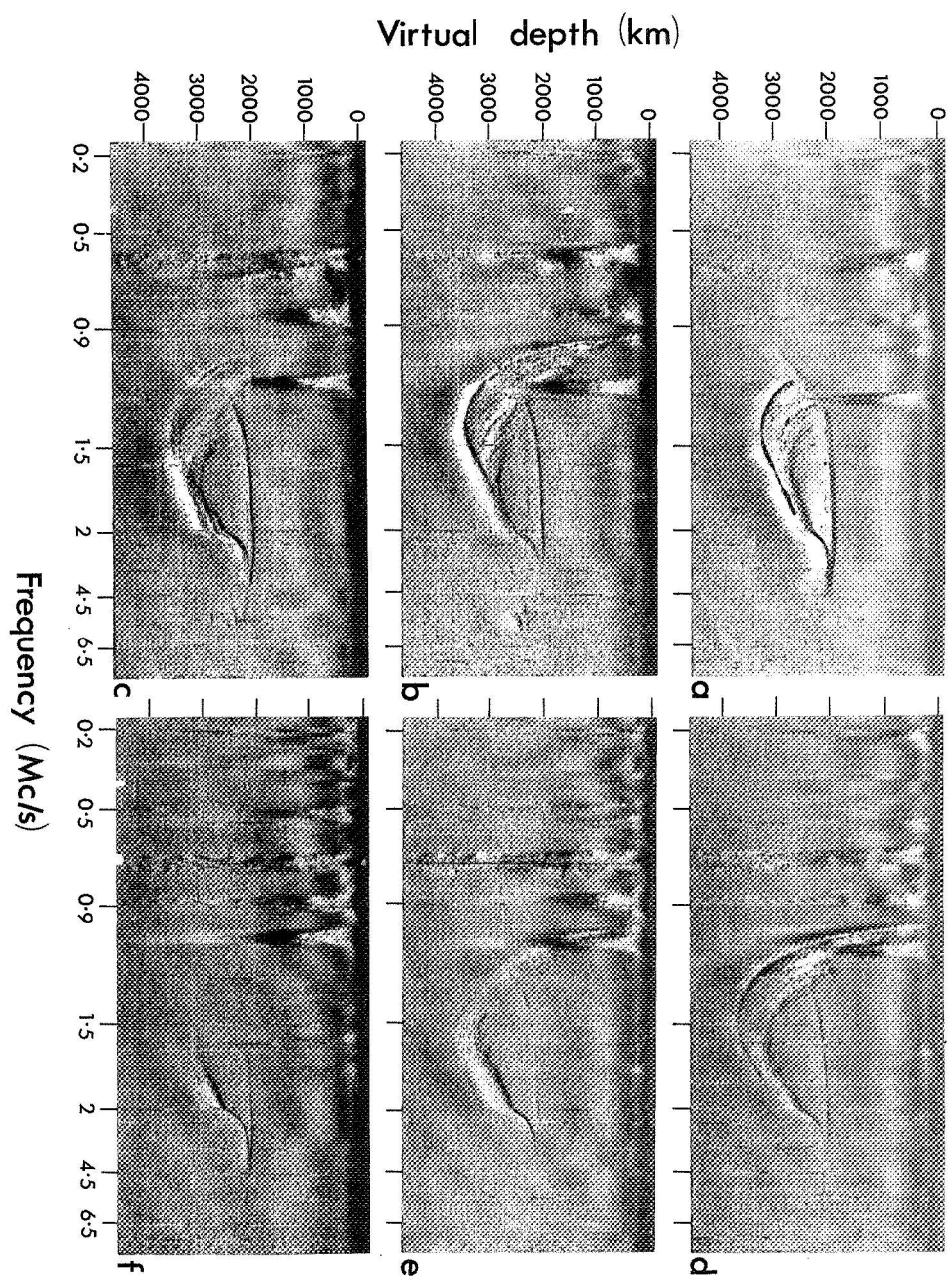


PLATE No: 25

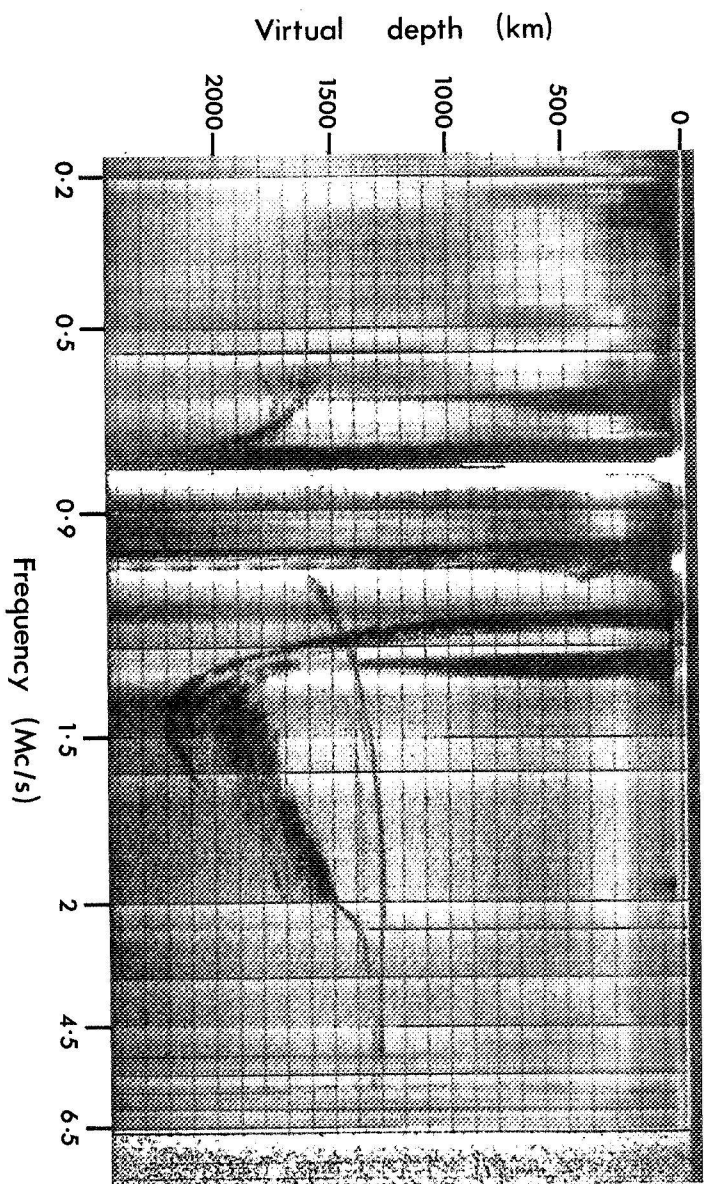


PLATE No: 26

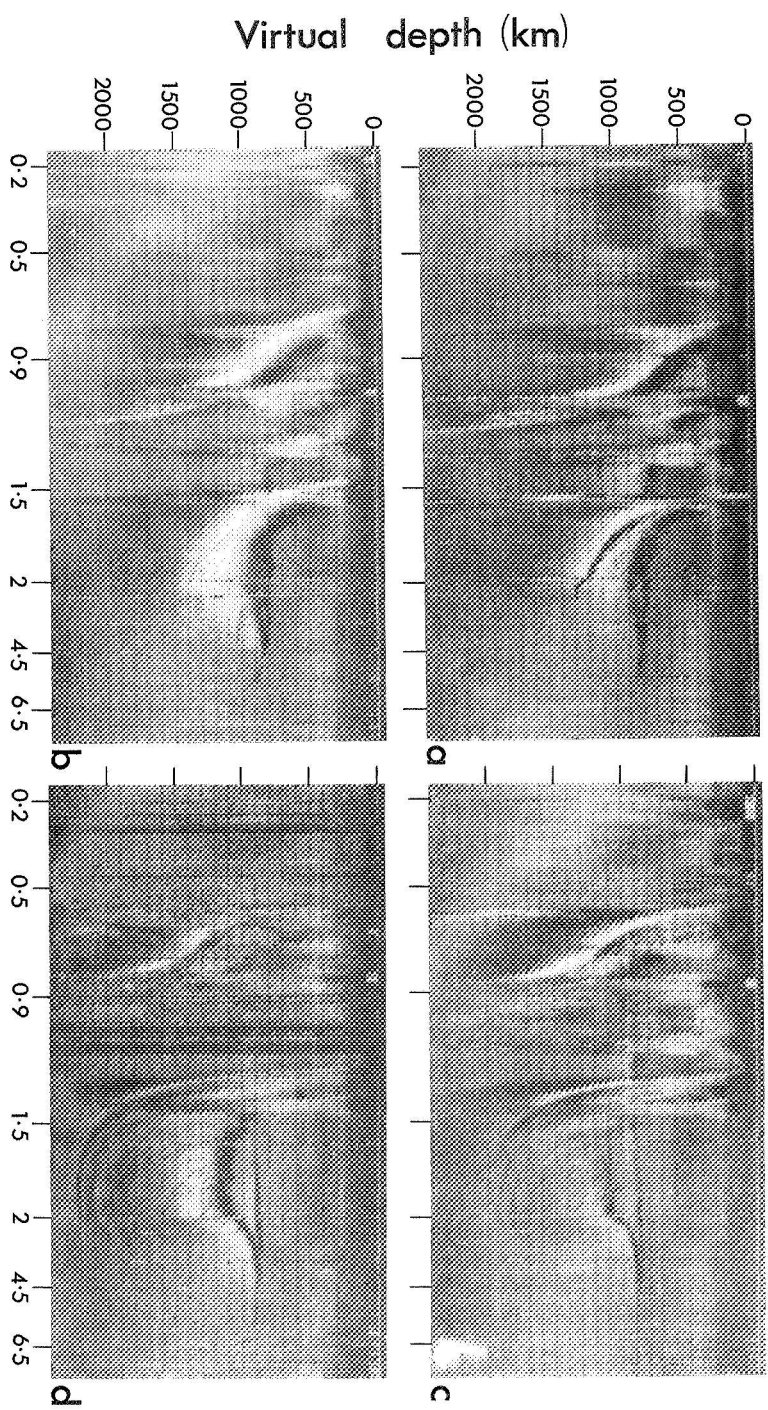


PLATE No: 27

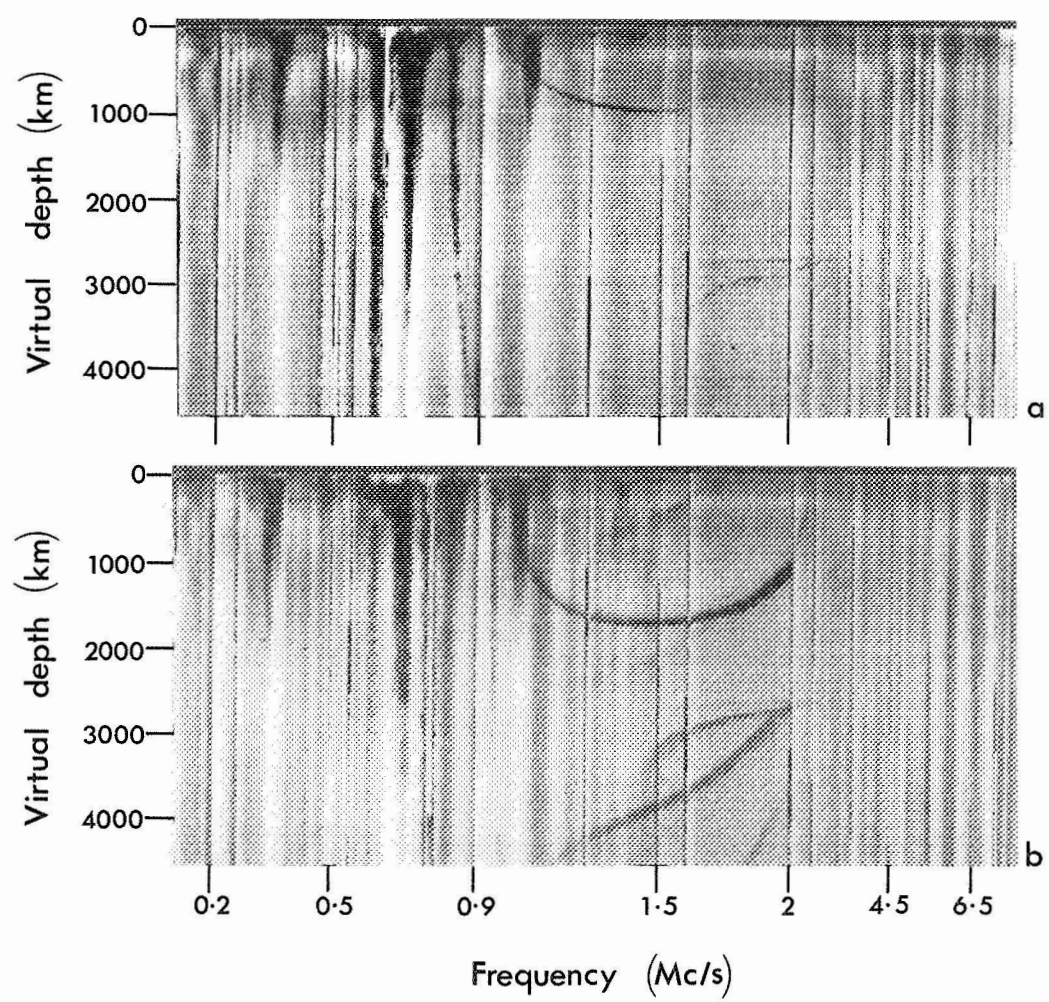


PLATE No:28

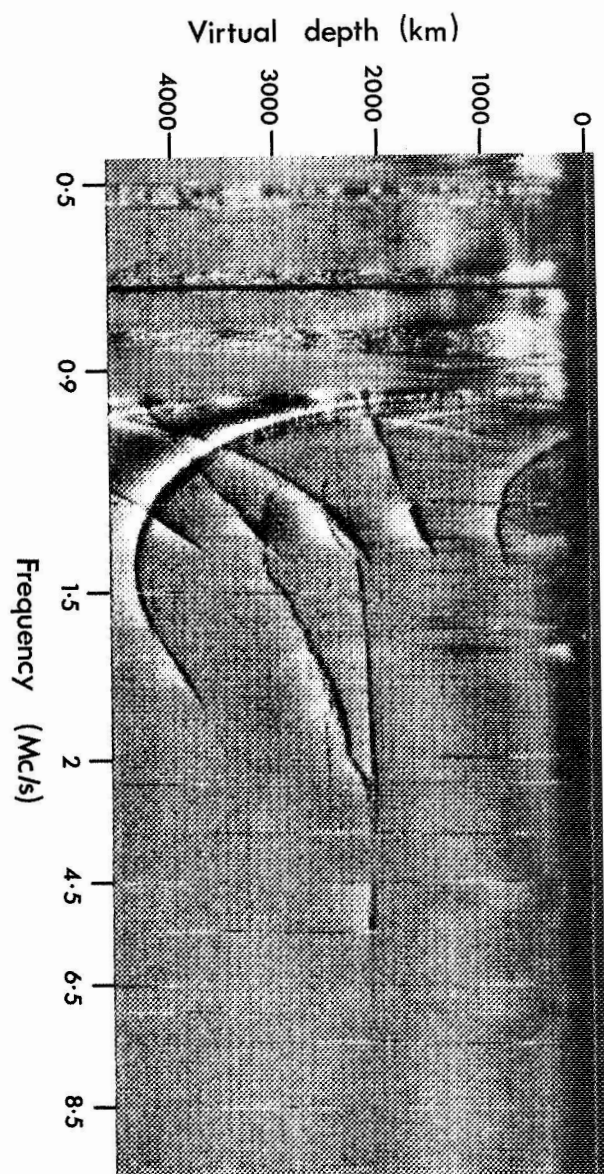


PLATE No: 29

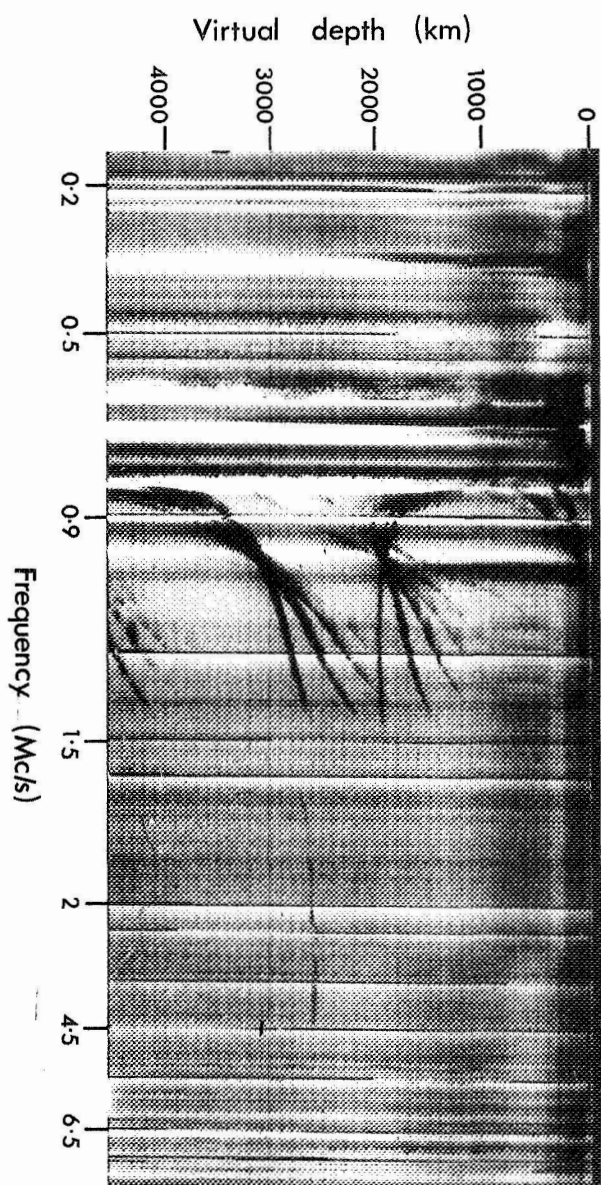


PLATE No: 30

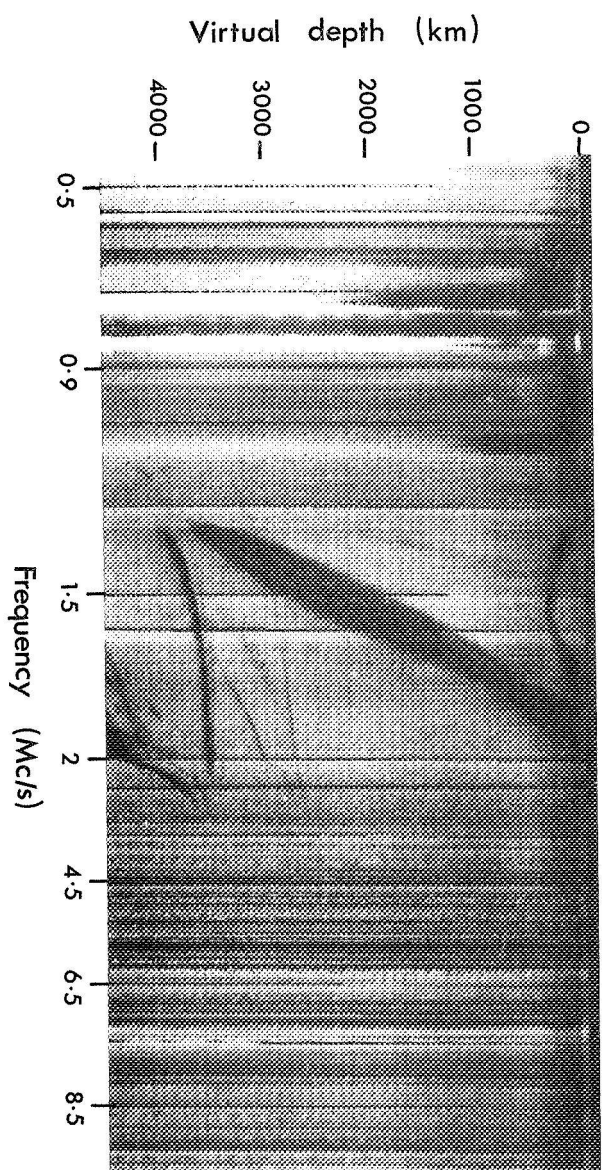


PLATE No : 31

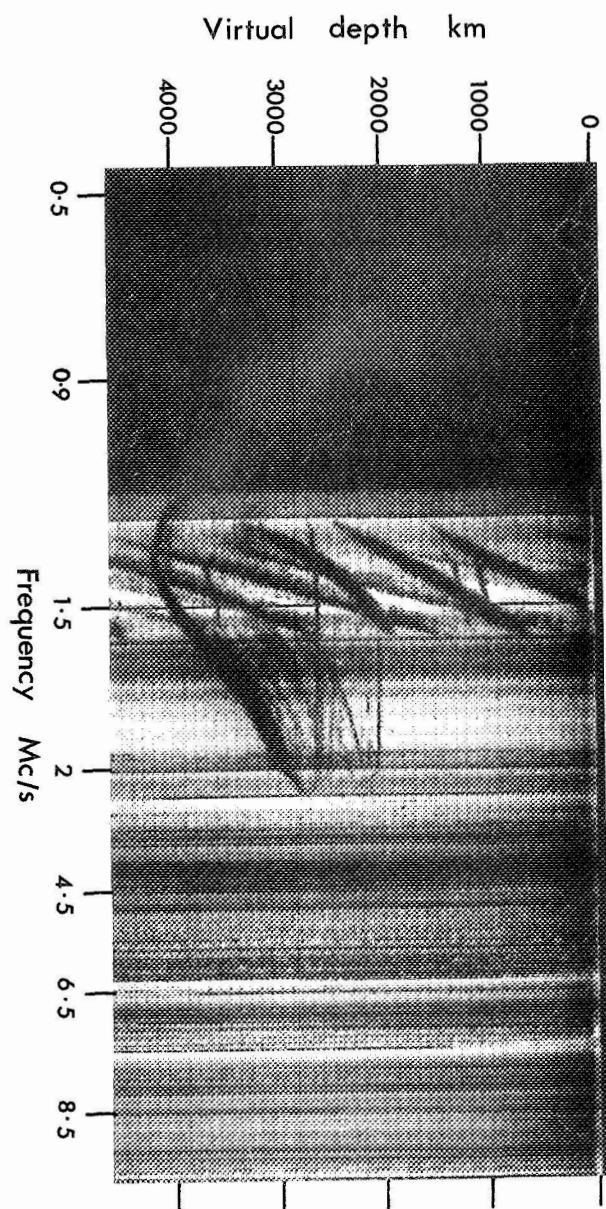


PLATE No : 32

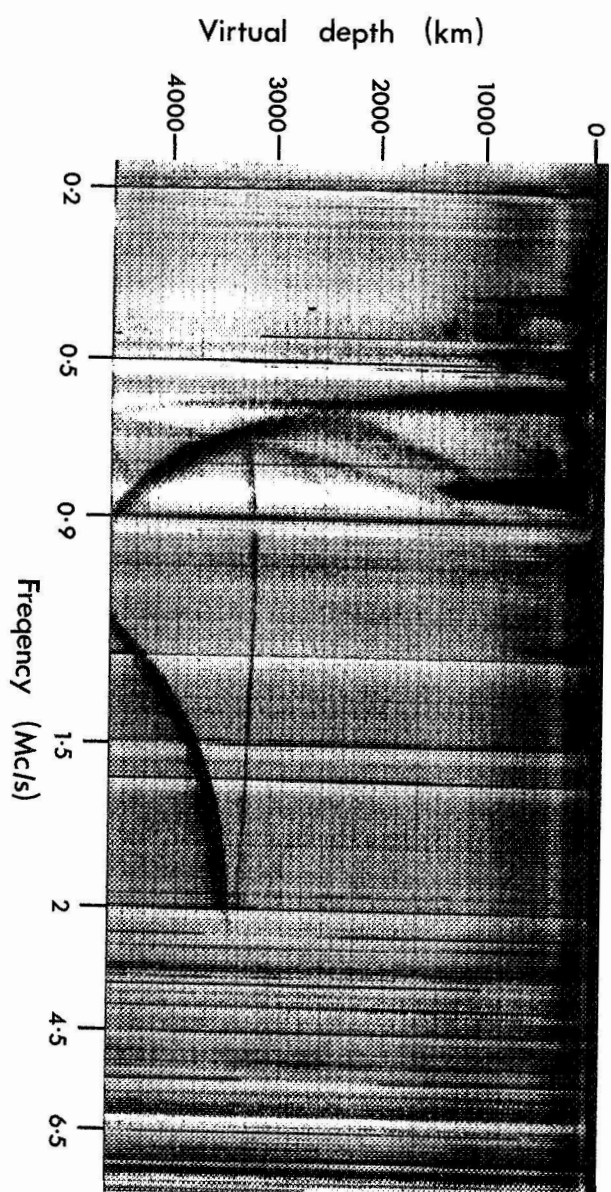
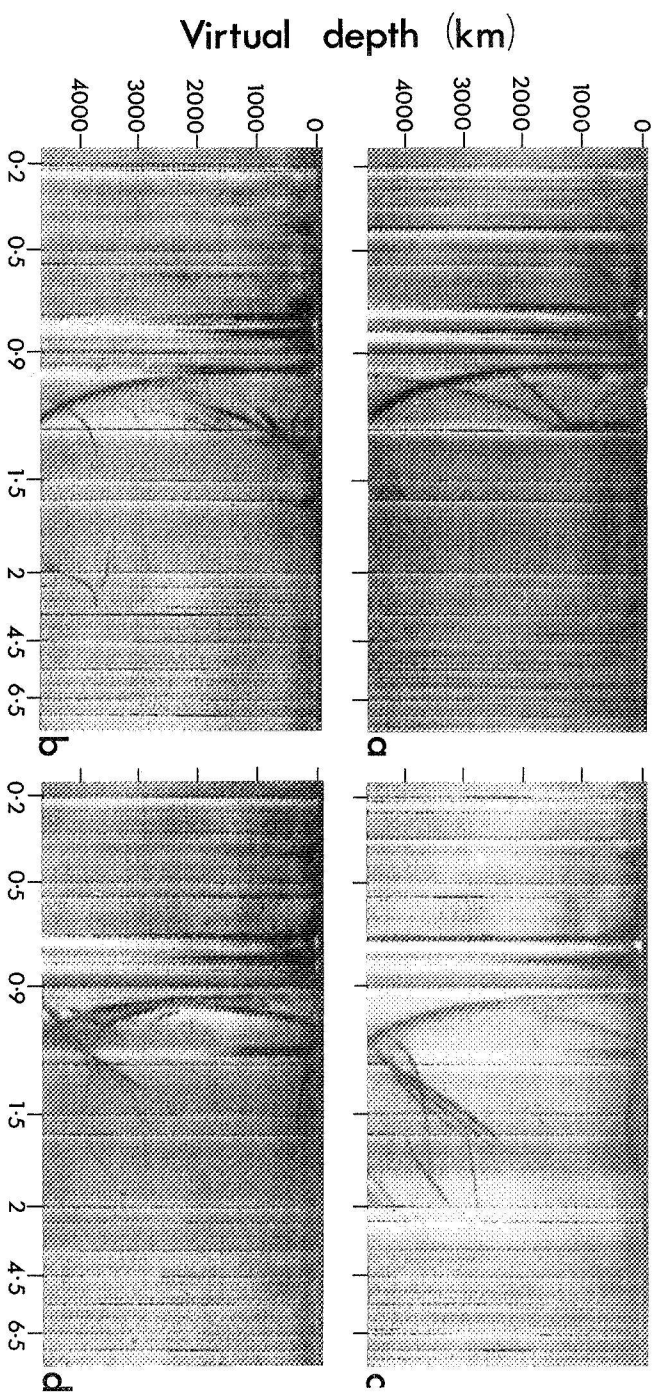
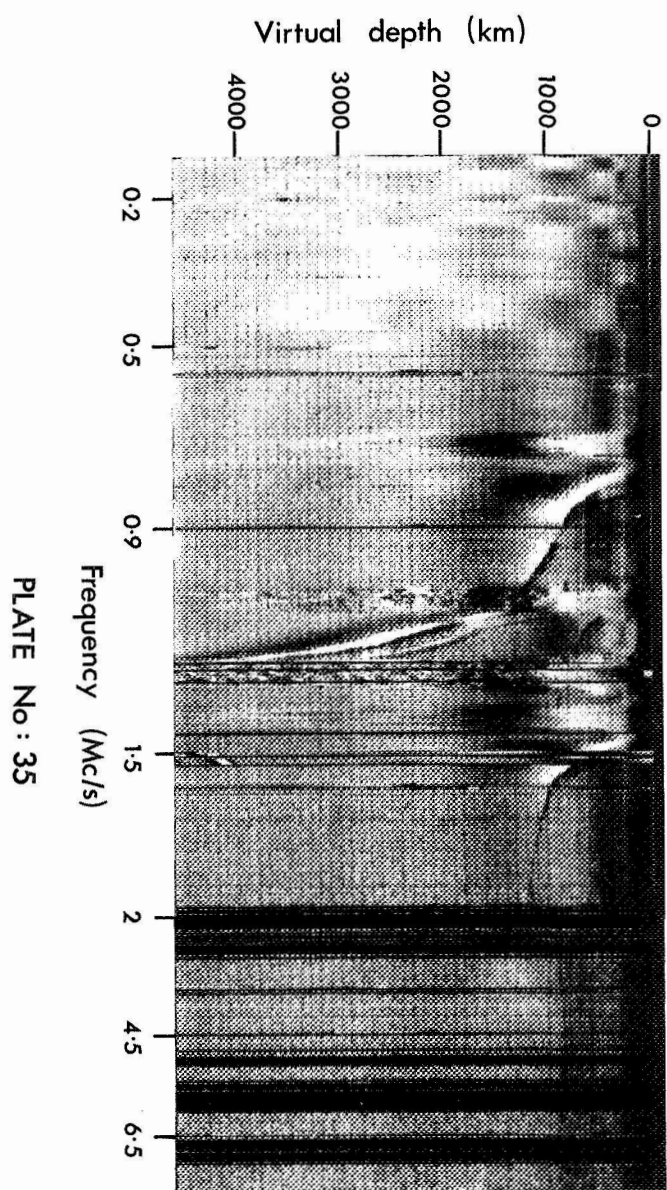


PLATE No: 33



Frequency (Mc/s)

PLATE No: 34



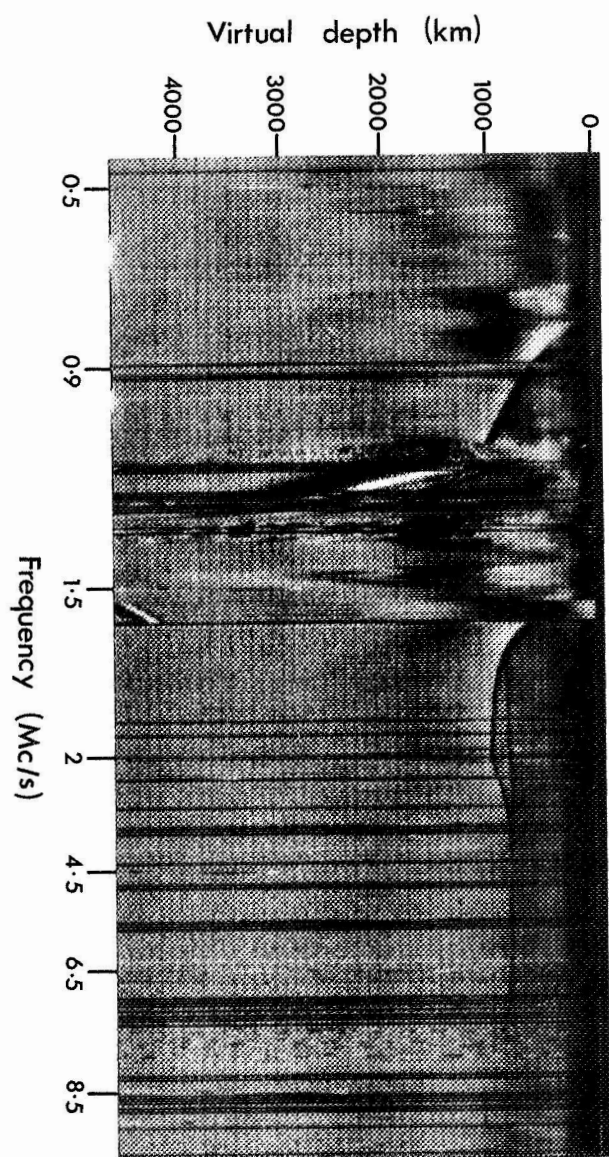


PLATE No: 36

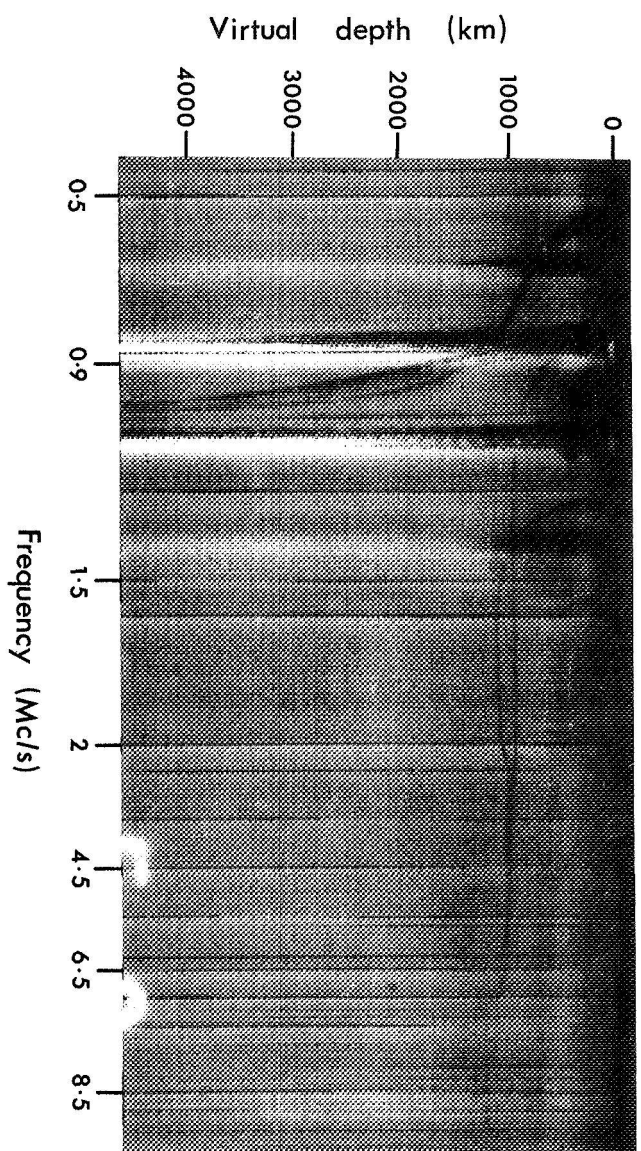


PLATE No: 37

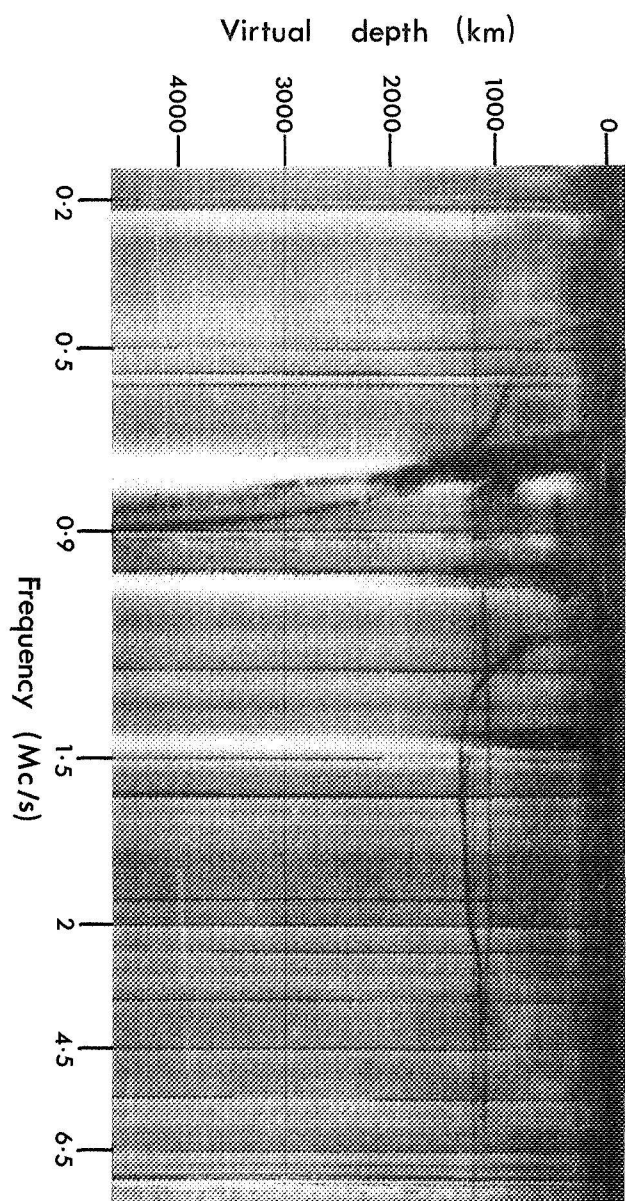


PLATE No:38

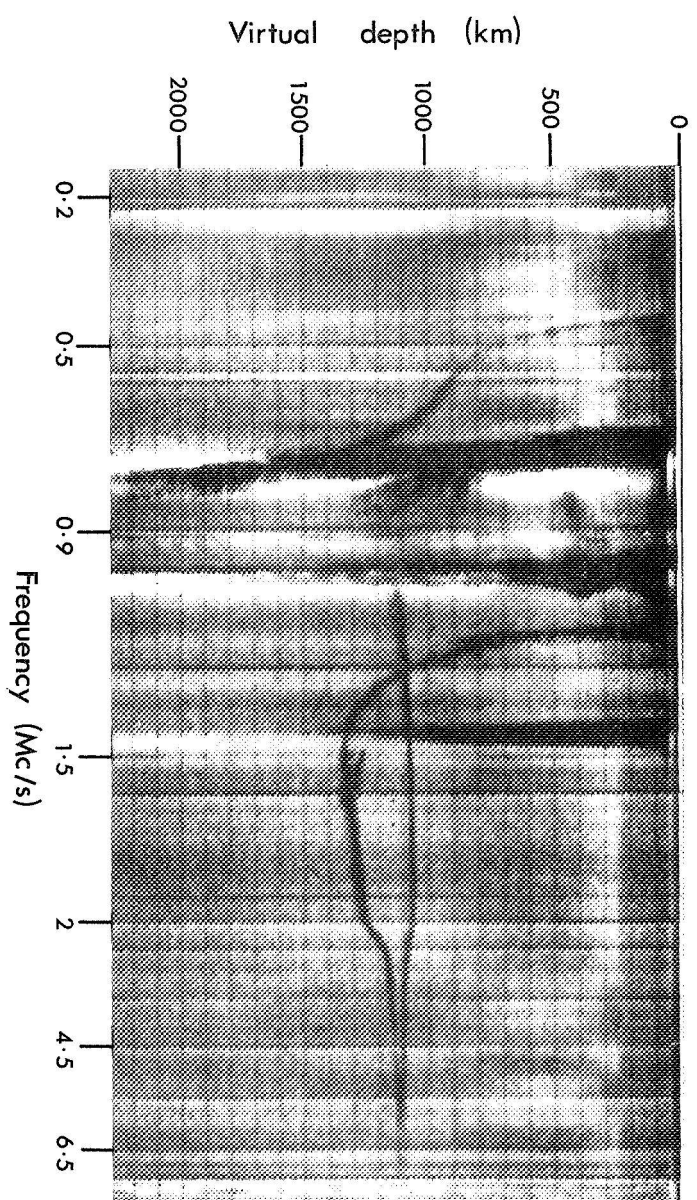


PLATE No:39

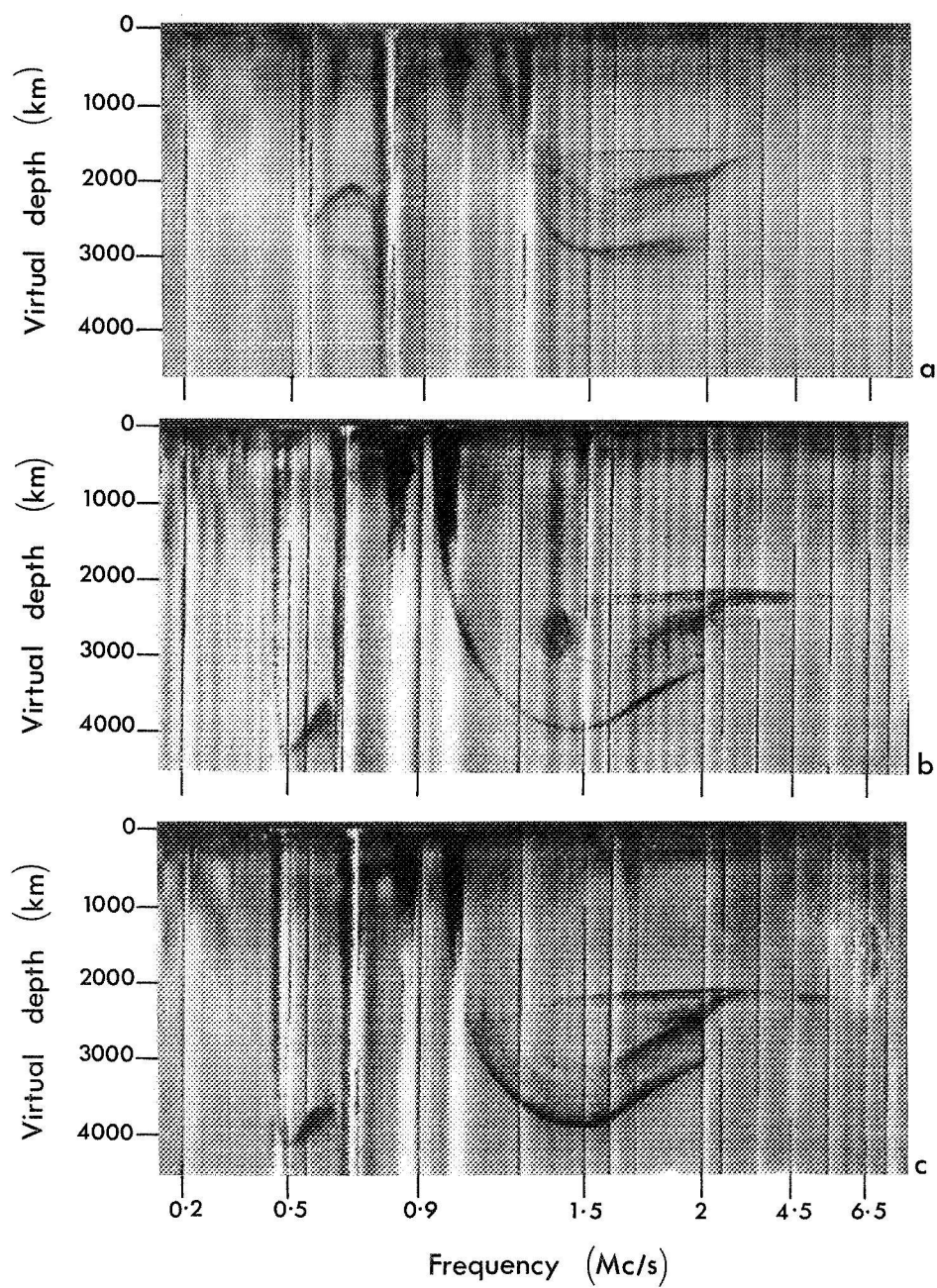


PLATE No: 40

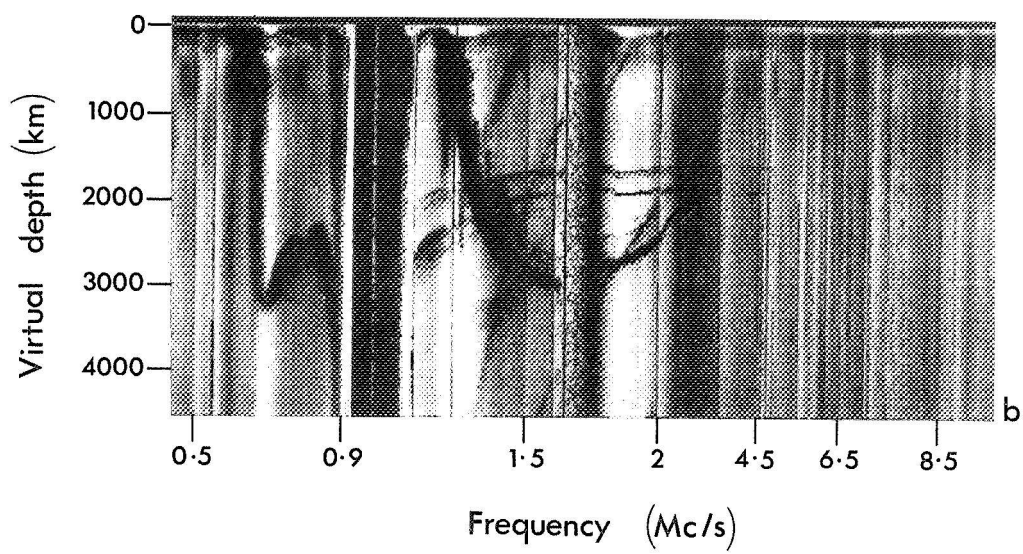
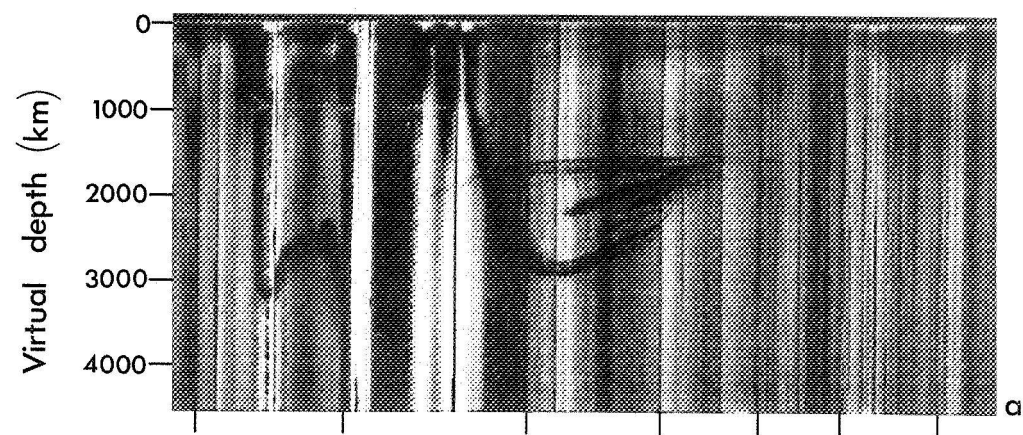


PLATE No: 41

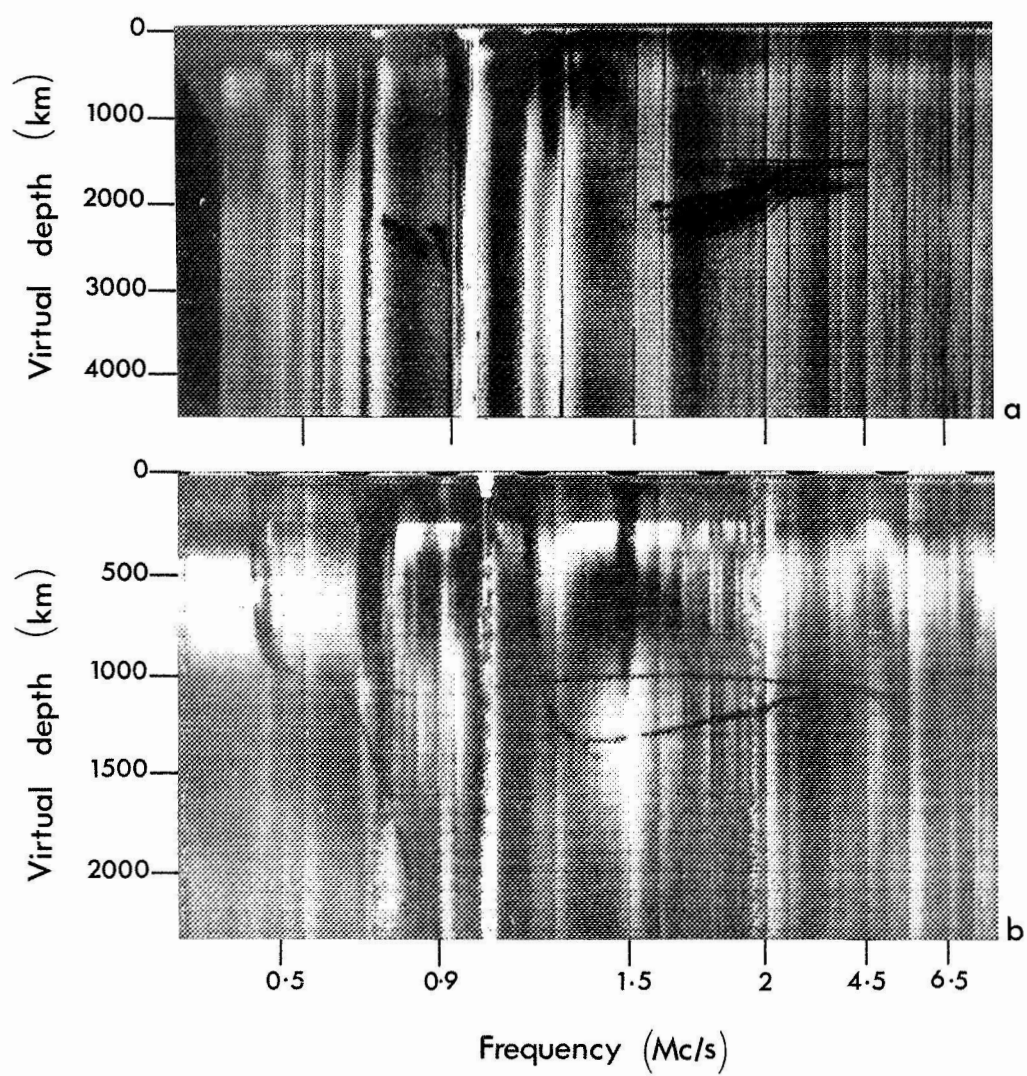


PLATE No:42

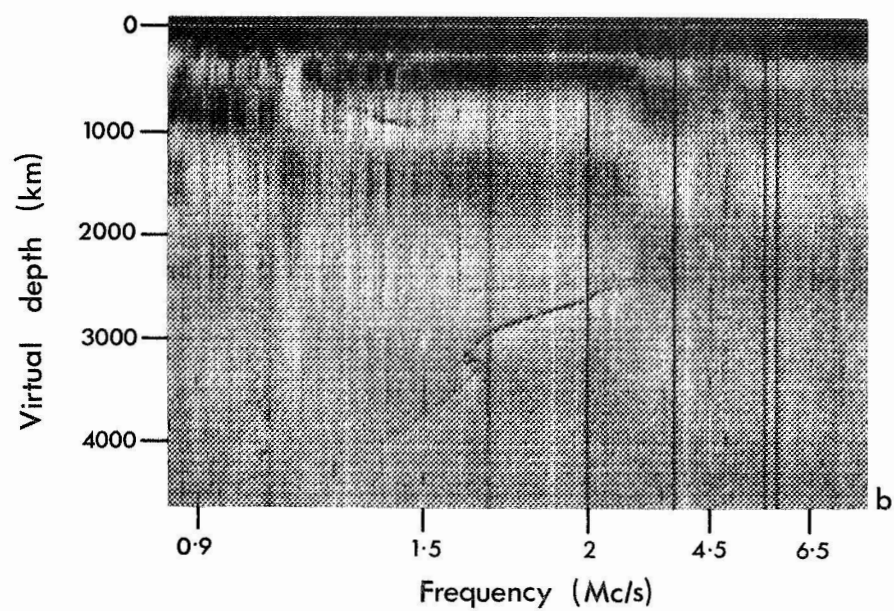
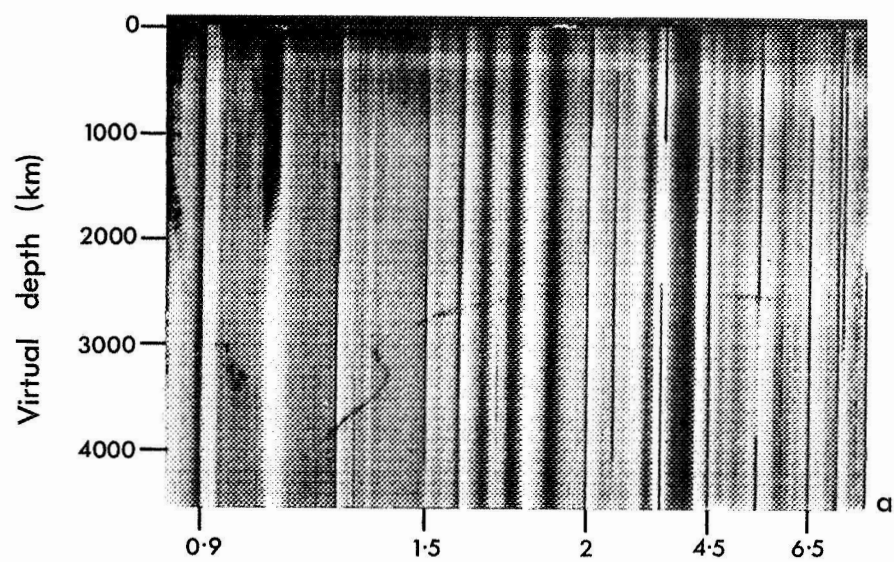


PLATE No: 43

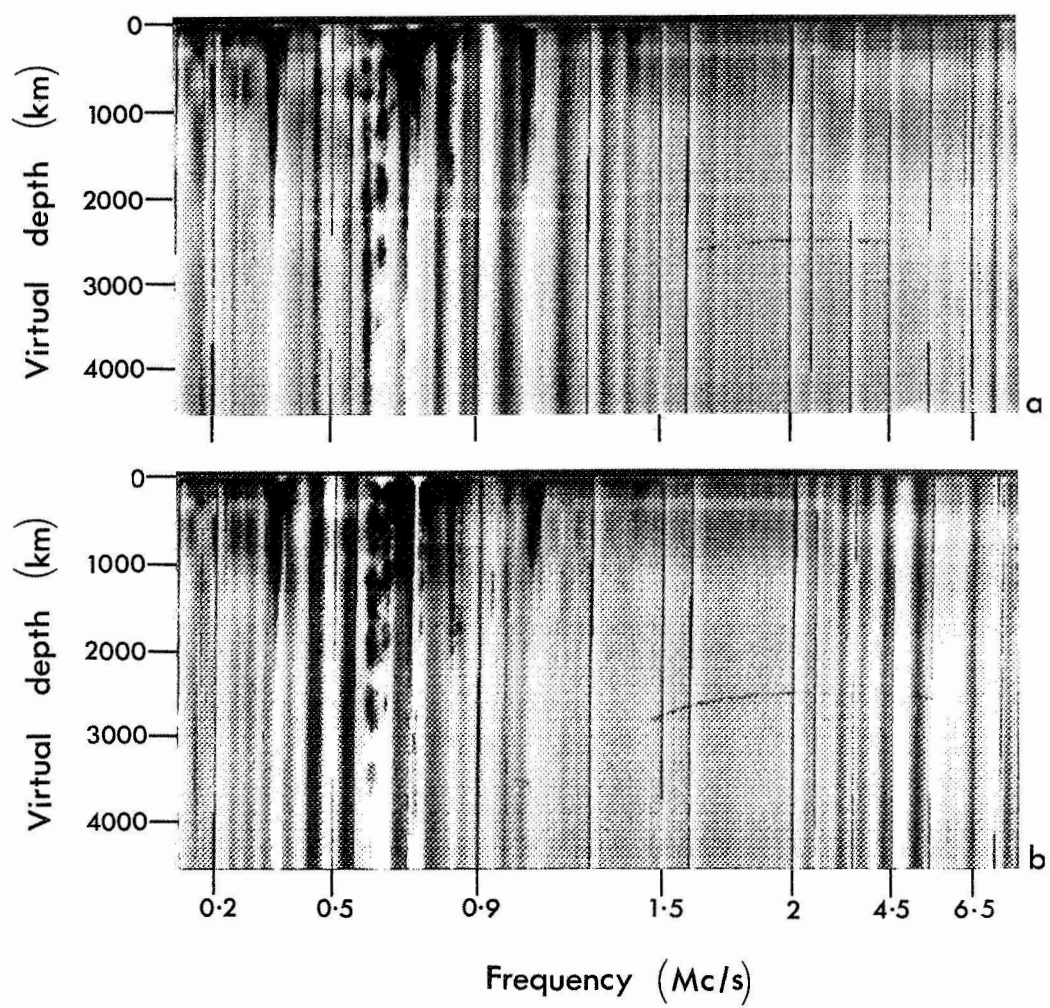


PLATE No:44

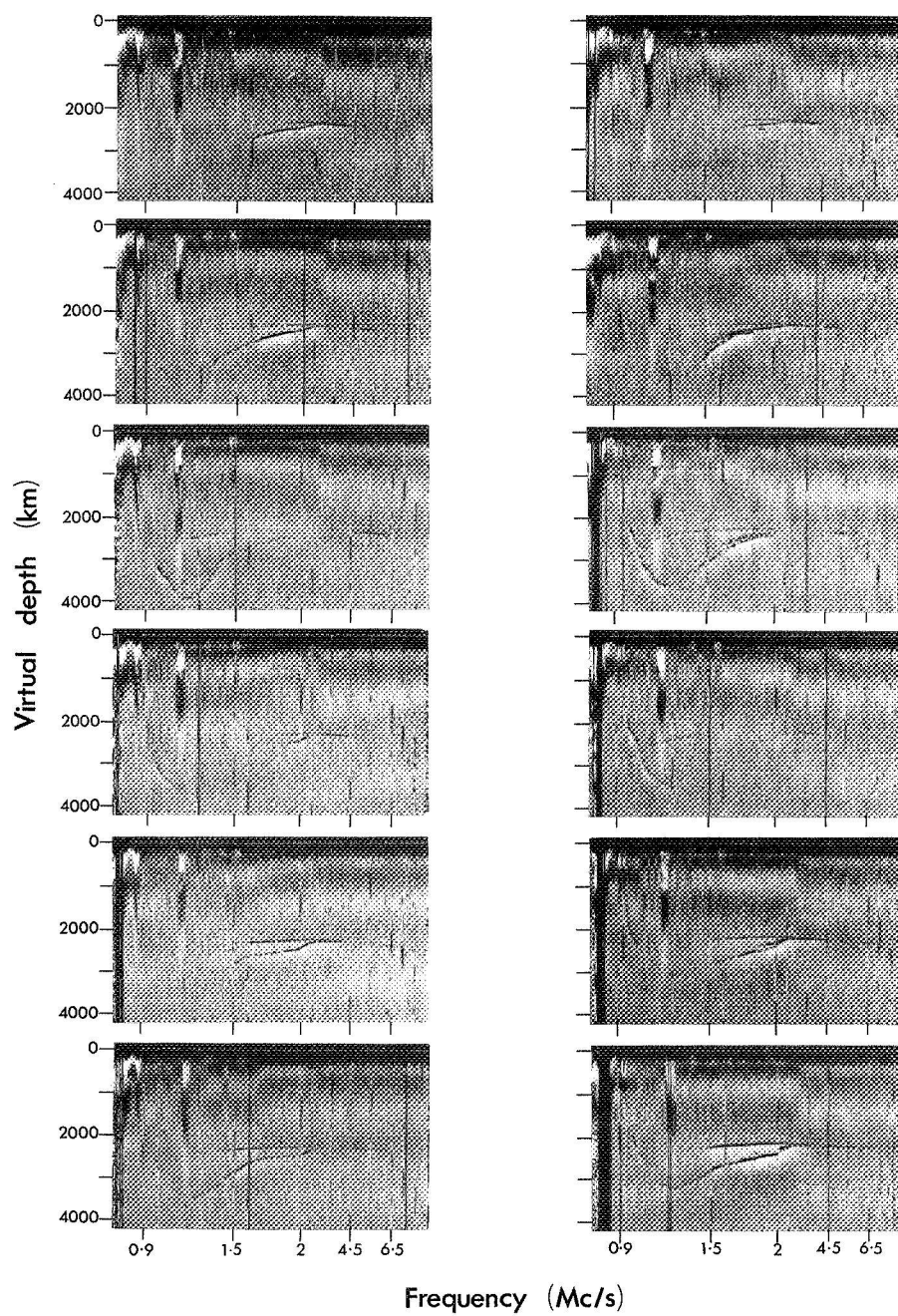
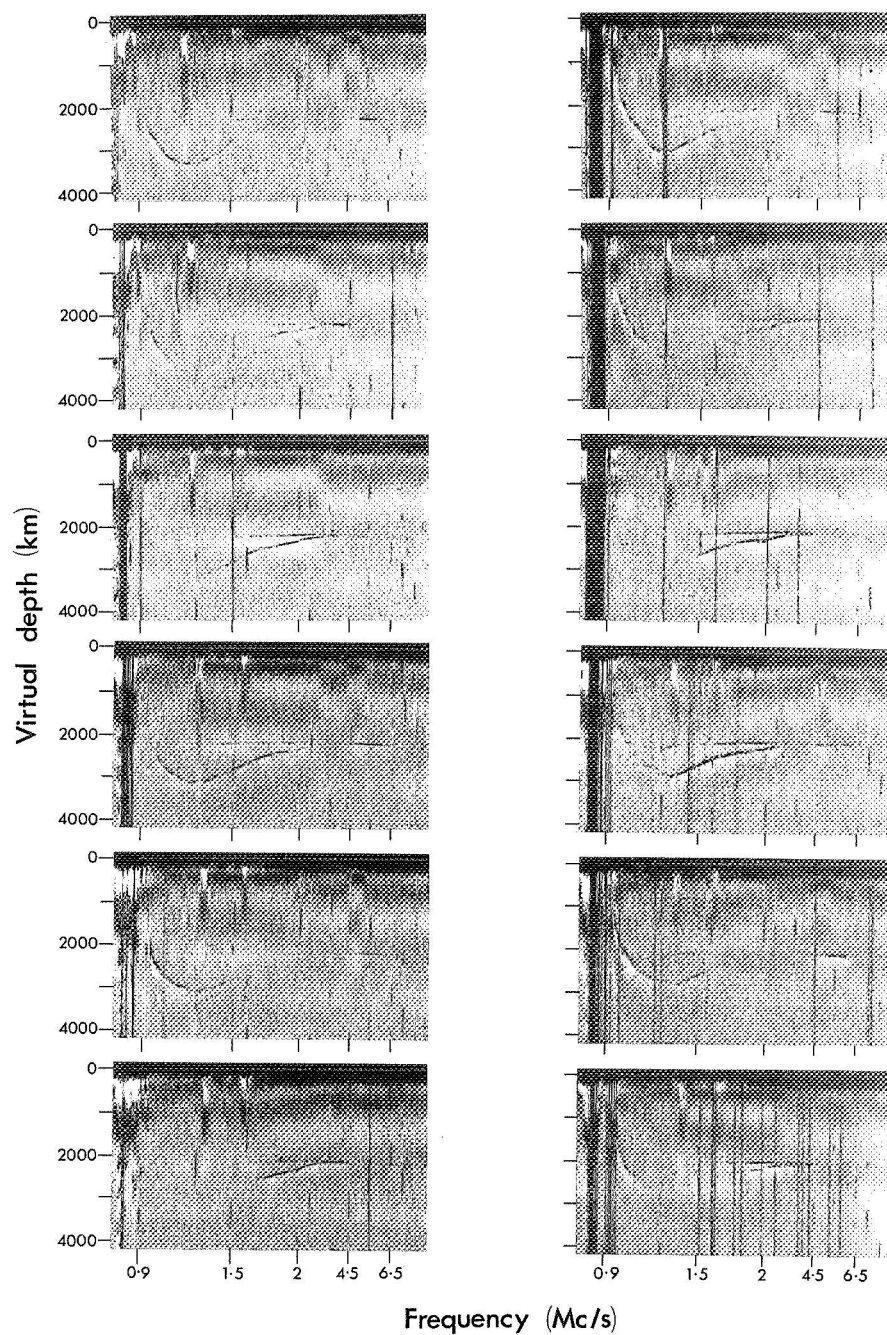
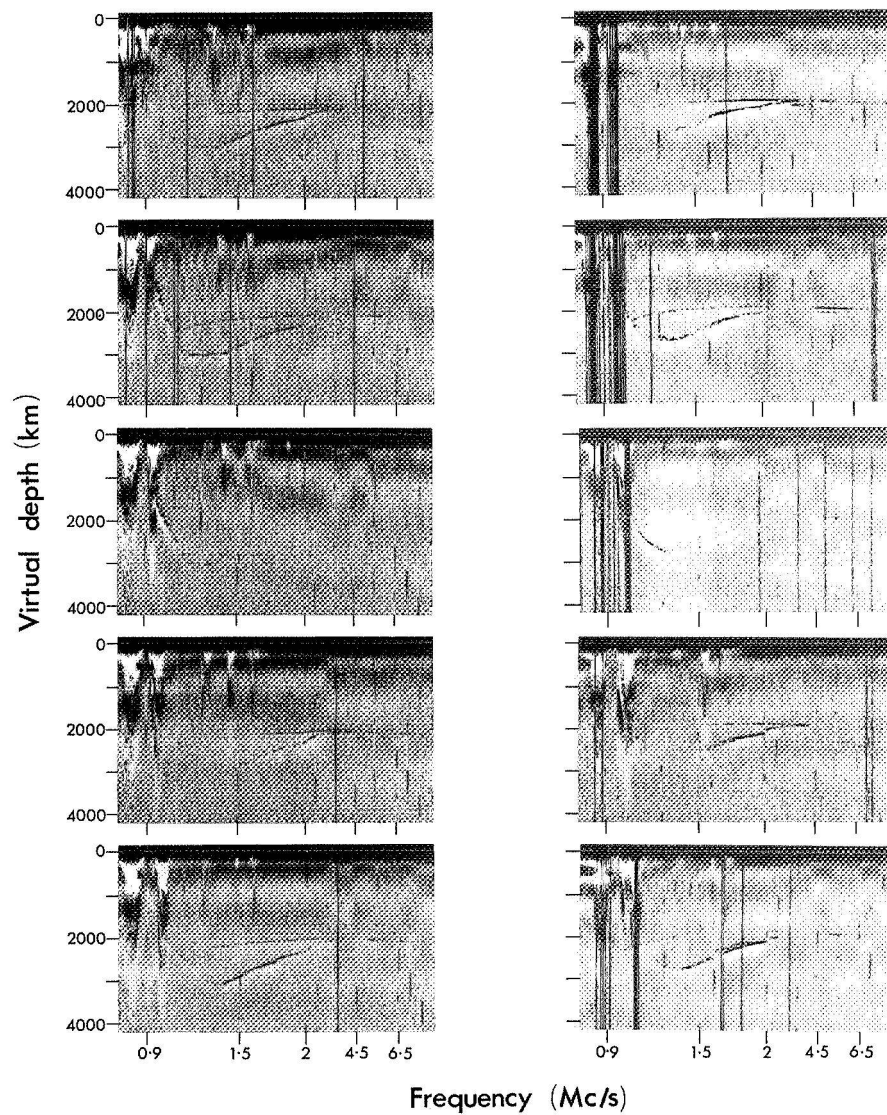


PLATE No:45



Frequency (Mc/s)

PLATE No:46



Frequency (Mc/s)

PLATE No: 47